Combined experimental and numerical kinetic characterization of NR vulcanized with sulfur, *N*-terbutyl, 2-benzothiazylsulfenamide, and *N,N*-diphenylguanidine

G. Milani,[1] T. Hanel,[2] R. Donetti,[2] F. Milani[3]

[1]Politecnico Di Milano, Piazza Leonardo Da Vinci 32, Milan 20133, Italy
[2]Pirelli Tyre, via Alberto E Piero Pirelli 25, Milan 20126, Italy
[3]Chem. Co. Consultant, via J.F.Kennedy 2, Occhiobello RO 45030, Italy
Correspondence to: G. Milani (E-mail: gabriele.milani@polimi.it)

ABSTRACT: A comprehensive experimental and numerical analysis aimed at investigating the rheometer behavior of Natural Rubber (NR) vulcanized with sulfur and two accelerators [*N,N*-diphenylguanidine (DPG) and *N*-terbutyl, 2-benzothiazylsulfenamide (TBBS)] is presented. To fit experimental data, the general reaction scheme proposed by Han and co-workers for vulcanized sulfur NR is re-adapted and suitably modified, taking into account DPG and TBBS single contributions. An *ad hoc* interactive software based on GUI technology is utilized to fit experimental data, allowing estimating kinetic constants also by unexperienced users. Chain reactions initiated by the formation of macrocompounds responsible for the formation of the instable crosslinked polymer are accounted for. In the presence of two accelerators, reactions are assumed to proceed in parallel, making the hypothesis of negligible interactions, being their concentrations rather similar. From the kinetic scheme adopted, a closed form solution is found for the crosslinking density, with the only limitation that the induction period is excluded from computations. © 2016 Wiley Periodicals, Inc. J. Appl. Polym. Sci. **2016**, *133*, 43519.

INTRODUCTION

The deep knowledge of the actual kinetics at the base of both Natural (NR) and Synthetic Rubbers cured with sulfur and accelerants is still an open issue. This is probably the reason why, despite the first utilization of vulcanized NR dates back to the second half of 19th century, the development of efficient numerical tools to predict the crosslinking degree achieved in standard curing conditions still remains a very challenging task.

As commonly accepted, the most diffused laboratory methodology to provide a macroscopic estimate of the crosslinking degree is the rheometer test. A rheometer is a laboratory device constituted by a chamber with either a fix and a moving part (MDR) or an oscillating disc inside (ODR), where a small rubber sample is cured at constant cure temperature and the torque applied to maintain a constant rotation of the moving part (moving die or oscillating disc) is measured.

A common feature exhibited by NR cured with sulfur is that the torque generally slightly decreases during a so called "induction" period of time, followed by a quite fast increase. Very frequently, in presence of sulfur, reversion is observed, which consists in a drop of the measured torque for relatively long curing times. Typically, reversion occurs for high vulcanization temperatures and the phenomenon is commonly thought to be a consequence of the degradation of polysulfidic (S-S or more) crosslinks.[1–4]

In practice, it has been observed that the importance of the reversion depends strictly on curing temperature. Nevertheless, recent results, for example, by Leroy *et al.*[5] and Milani *et al.*[6–8] have shown that the ratio between thermally stable (short) and unstable (long) polysulfidic crosslinks is temperature dependent, but much more important turns out sulfur and accelerators concentration.

The literature in the field of NR vulcanized with sulfur is certainly dated and superabundant, especially from an experimental point of view.[9–11] However, the kinetic models at present available cannot be considered fully exhaustive and for sure do not adapt to any compound that can be potentially encountered in practice. As a matter of fact, some of them are only phenomenological, essentially basing on experimental torque curve fitting,[6,12] whereas some others take into consideration only a few (the most important) chemical reactions occurring during sulfur curing.[13,14] The

first family is thus unsuitable when a prediction of the crosslinking density is needed at temperature conditions different from those experimentally tested, whereas the second one may provide incorrect evaluations of the kinetics constants when various compounds of polymer with different additives, carbon black, sulfur, and accelerators are present.

Existing models allowing a prediction of NR mechanical behavior through the kinetics of rubber vulcanization, by means of either mechanistic (Coran,[4] Ding and Leonov[13,14]) or semimechanistic (Han et al.[15]) base, suffer from important limitations, such as the need of evaluating kinetic constants by best fitting numerical procedures on the available experimental data and the generalist point of view, which does not take into account the actual accelerators present in the system.

Recently, Leroy et al.[5] derived a phenomenological model with the same formalism of Han et al.[15] and Colin et al.,[16] which gives a continuous prediction of the induction/vulcanization/reversion sequence. Similar approaches following the same scheme may be also found in Milani and Milani[6] and Milani et al.[7] Essentially, the phenomenological model proposed by Leroy et al.[5] assumes that during the induction and vulcanization steps, the overall formation of sulfur crosslinks can be described by a classic Kamal and Sourour formulation,[12] which supposes a catalytic and autocatalytic second order apparent reaction mechanism. The procedure has been recently refined by Milani et al.,[7] where a complex kinetic scheme with seven constants has been proposed, describing reversion by means of the distinct decomposition of single/double and multiple S-S bonds. Finally, the authors of this article specialized Han's model in presence of two accelerators,[17] whereas Milani and Milani[18] have recently proposed an original approach to by-pass best fitting in Han's model, with a recursive determination of the kinetic constants by means of an iterative approach which can be handled with commercial spreadsheets.

Aim of the present article is to push the research forward in the field of NR sulfur vulcanization by means of a comprehensive experimental and numerical approach. The experimental campaign is carried out on a NR compound prototype exclusively constituted by NR, zinc octoate, sulfur and two accelerators [N-terbutyl, 2-benzothiazylsulfenamide (TBBS) and N,N-diphenylguanidine (DPG)]. On such particular benchmark compound, the experimental campaign in rheometer is conducted varying (1) vulcanization temperature (four curing temperatures, namely 150, 160, 170, and 180 °C, have been investigated) and (2) mutual concentrations of S, TBBS and DPG.

Basing on the experimental results obtained, a modification of the mathematical model proposed by Han and already presented by the authors[17] is implemented in an interactive software based on Graphical User Interface (GUI) technology, where the optimization of the numerical approach on experimental data is not performed with standard best fitting, but by means of a very intuitive trial and error procedure, favored by the interaction of the program with the user by means of sliders.

The numerical model essentially relies into a GUI that can be managed even with unexperienced users and which allows an estimation of kinetic constants, to be used with predictive purposes outside the range of concentrations inspected, without the need of any particular optimization routine.

As a matter of fact, the predictive capabilities are assessed by a twofold check: the first is done on the crude experimental data. It is indeed found that, for all the cases inspected, the numerical model always fits rather well experimental rheometer curves. The second check can be done assessing if the kinetic constants found at the four curing temperatures experimentally investigated reasonably obey an Arrhenius law (i.e., the values of the logarithm of the kinetic constants plotted against the inverse of the absolute temperature do not deviate from a straight line) providing useful hints on the effects induced by both cure temperature and an increase in concentration of a particular ingredient. As pointed out by Prigogine,[19] the function drives the crosslinking structure, meaning that any numerical model proposed can be regarded as an interpretation of the crosslinking system, allowing for a prediction of rubber macroscopic behavior.

The kinetic model bases on the general reaction scheme proposed by Han and coworkers for vulcanized sulfur NR, which is consistently modified accounting for the single contributions of the different accelerators. Chain reactions initiate by the formation of macrocompounds that are responsible for the formation of stable and unstable crosslinked polymer. It is assumed that such reactions depend on the reciprocal concentrations of all components and their chemical nature. In the presence of two accelerators, reactions are assumed to proceed in parallel, making the assumption that there are no cross-reactions between the two accelerators. This assumption is fully justified by the statistical results regarding the interaction parameters on linear and non-linear meta-models presented by the authors in a companying article.[20]

A synoptic critical analysis of the numerical (kinetic constants) and experimental results obtained is finally reported at the end of this article.

EXPERIMENTAL

The experimental campaign is conceived and designed by the authors to investigate the response of a pre-defined rubber compound with known characteristics under variable concentrations of S, TBBS, and DPG.

The NR formulation used is presented in Table I.

To properly mix and homogenize all ingredients, an internal mixer maintained at nearly 50 °C as recommended by ASTM D3184–11[21] has been used.

Natural Rubber (SMR–20) has molecular weight by number $M_n = 1.5 \times 10^5$ and polydispersity of 6.3 (measured by gel permeation chromatography), with density of 917 kg/m^3.

Table I. NR Formulation Used in the Experimental Campaign

Ingredients (phr)	S, TBBS	S, TBBS	S, TBBS	S, TBBS
	1, 1	3, 1	3, 3	1, 3
DPG	1	1	1	1
DPG	2	2	2	2
DPG	3	3	3	3
DPG	4	4	4	4
NR	100	100	100	100
$C_{16}H_{30}O_4Zn$ Zinc Octoate	3	3	3	3

The accelerators used are TBBS (Industrial name Westco TBBS) from Western Reserve Chemical, DPG from Carlo Erba Reagents and sulfur powder from Gasoilsulfur.
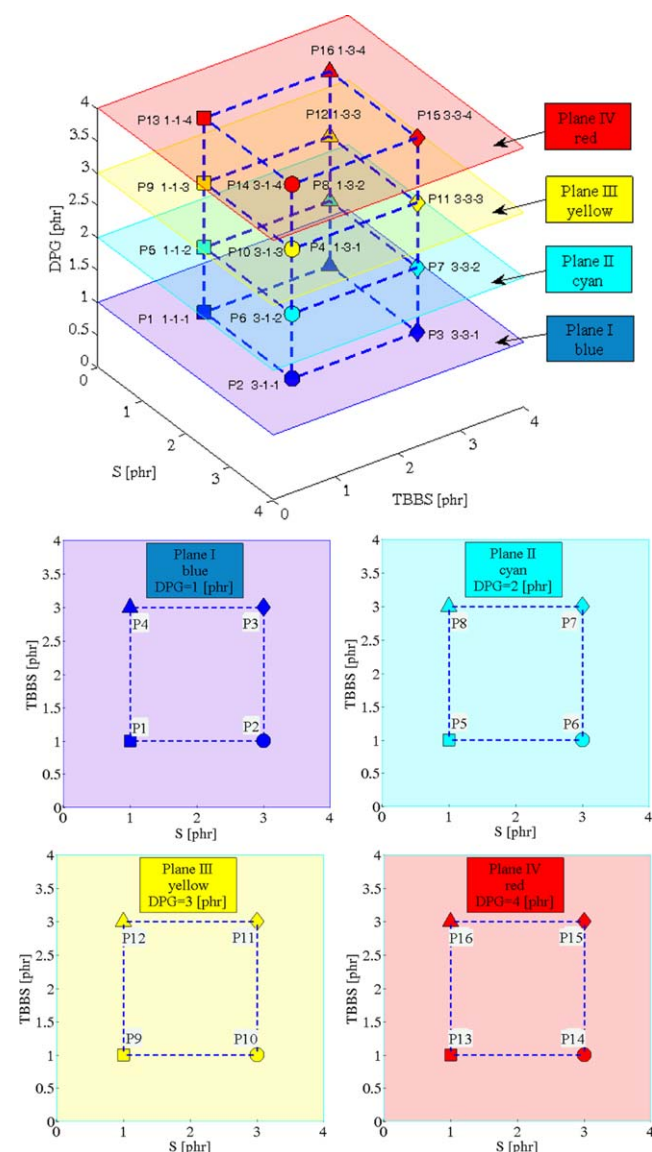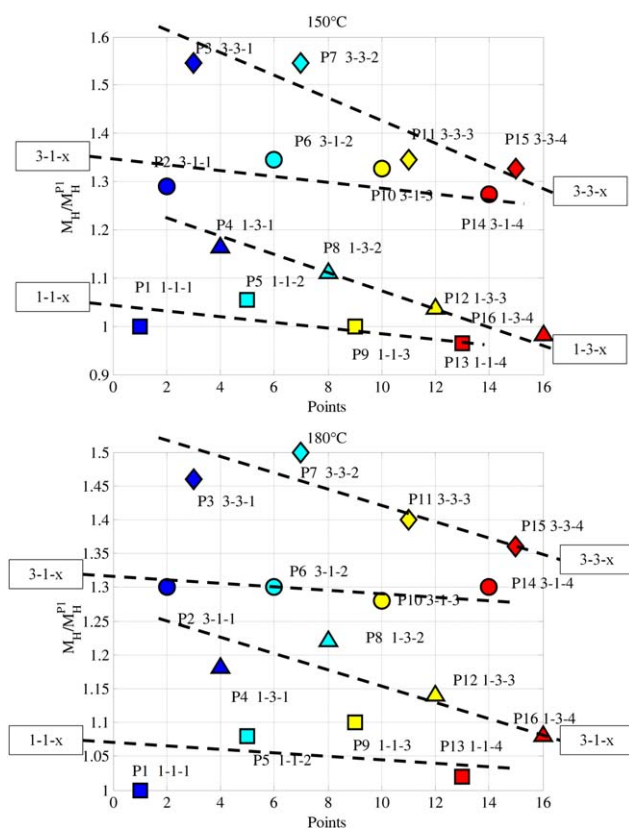

Figure 1. Sensitivity scheme of the experimental analyses conducted using S-TBBS-DPG at different concentrations. [Color figure can be viewed in the online issue, which is available at wileyonlinelibrary.com.]
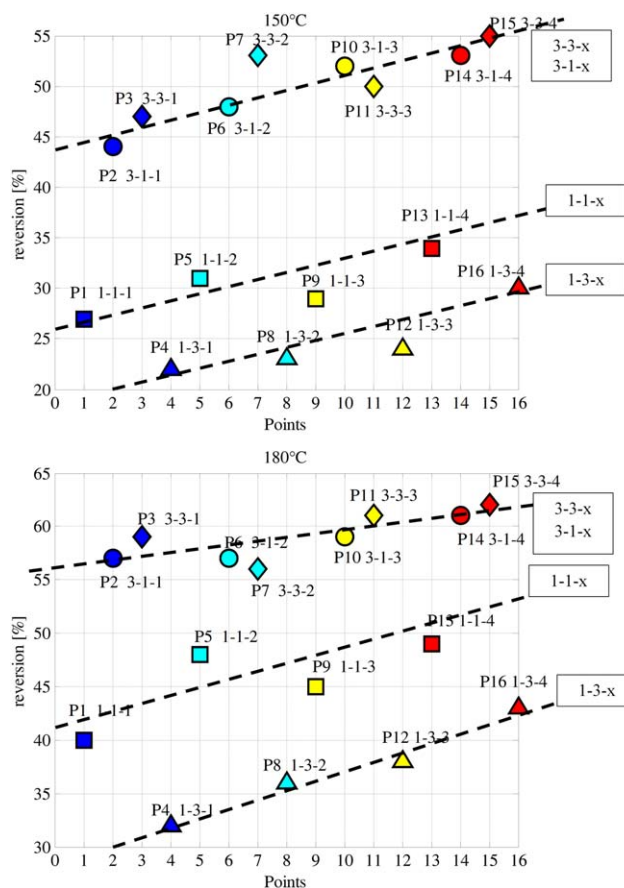
Figure 2. Experimental reversion % at 150 °C (top) and 180 °C (bottom) as a function of S-TBBS-DPG concentration variations. [Color figure can be viewed in the online issue, which is available at wileyonlinelibrary. com.]

Rubber compounds have been conditioned at nearly 25 °C for 24 h prior curing on a Monsanto oscillating Disc Rheometer fulfilling requirements by ASTM D2084-81. The tests are carried out at four temperatures: 150, 160, 170 and 180 °C.

The experimental campaign is conducted following the sensitivity analysis scheme represented in Figure 1. Two concentrations of S have been considered, equal to 1 or 3 phr, two of TBBS, equal to 1 or 3 phr and four concentrations of DPG (1, 2, 3, 4 phr). In Figure 1, four superimposed parallelepipeds along DPG vertical axis (or analogously four horizontal planes I–IV at constant DPG concentration) are represented. Each corner, from P1 to P16, is a tested rubber sample with fixed S-TBBS-DPG concentration. On each of the four planes I–IV four experimental data points lay, having in common the same constant concentration of DPG. For instance, on Plane I points from P1 to P4 lay, all having a DPG concentration equal to 1 phr. It is worth noting that vertical edges of the parallelepiped with bases P1-P4 and P13-P16 are represented with different symbols. In particular, points having S-TBBS concentrations equal to 1-1, 3-1, 3-3, and 1-3 are depicted with squares, circles, rhombs and triangles respectively. The color of the symbol on the relevant edge classically passes from blue to red representing from low to high concentrations of DPG. The color of the symbols corresponds to

Figure 3. Experimental normalized maximum torque (M_H) at 150 °C (top) and 180 °C (bottom) as a function of S-TBBS-DPG concentration variations. [Color figure can be viewed in the online issue, which is available at wileyonlinelibrary.com.]

the color of the plane considered, so that plane I (DPG = 1 phr) collects blue tested points, plane II (DPG = 2 phr) cyan points, plane III (DPG = 3 phr) yellow points, and plane IV (DPG = 4 phr) red points. A constant amount of Zn-octoate at 3 phr was also used as additive.

EXPERIMENTAL RESULTS

A synopsis of the huge amount of experimental results obtained in the present investigation is reported from Figures 2 to 6. The most important parameters of the experimental rheometer curves are represented for each point (from P1 to P16), namely reversion percentage, maximum torque M_H, CRI (i.e., cure rate index, defined as $100/(t_{90}-t_s)$, where t_{90} is the time at 90% of vulcanization), scorch time t_s, and time at maximum torque $t_{100}-t_s$.

When dealing with experimental reversion percentage evaluated at 180 and 150 °C, see Figure 2, it is worth noting a very clear trend with respect to concentrations of both S and accelerators. As expected, it turns out that the reversion percentage is linked to the curing temperature. As a matter of fact, at 150 °C the reversion is smaller in absolute terms. It seems also that reversion % tends slightly to "stabilize" for concentrations of DPG greater than 2, suggesting a sort of non-linear saturation effect in dependence of DPG concentration, which should be investigated with dedicated experimentation. DPG concentrations lower than 2 phr should be utilized in the reference compound

to strongly reduce the induction period and thus limiting to some extent reversion. Furthermore, it is worth noting that the model system here studied refers to an idealized compound constituted exclusively by rubber, zinc octoate, sulfur, and accelerants. This is suitable for research purposes, whereas in real cases of industrial interest DPG exhibits quite beneficial effects.

Regarding the evaluation of the maximum torque M_H, the reader is referred to Figure 3, where M_H experimentally obtained (normalized against maximum torque obtained for point P1, for which M_H is equal to 5.4, 5.2, 5.1, and 5.0 dNm at 150, 160, 170, and 180 °C, respectively) at 150 and 180 °C is depicted. When sulfur in high concentrations is utilized, the maximum torque obviously increases, because sulfur is directly proportional to transversal links between parallel chains. It is also observed that TBBS has a beneficial effect in increasing the torque, whereas there is no experimental evidence on a remarkable effect of DPG in increasing M_H (on the contrary, it seems to be associated to a slight decrease of the maximum torque, as shown in Figure 3, where red points—associated to DPG at the highest concentration—exhibit on average 10–15% lower values of the torque when compared with blue points—associated to DPG at the lowest concentration).
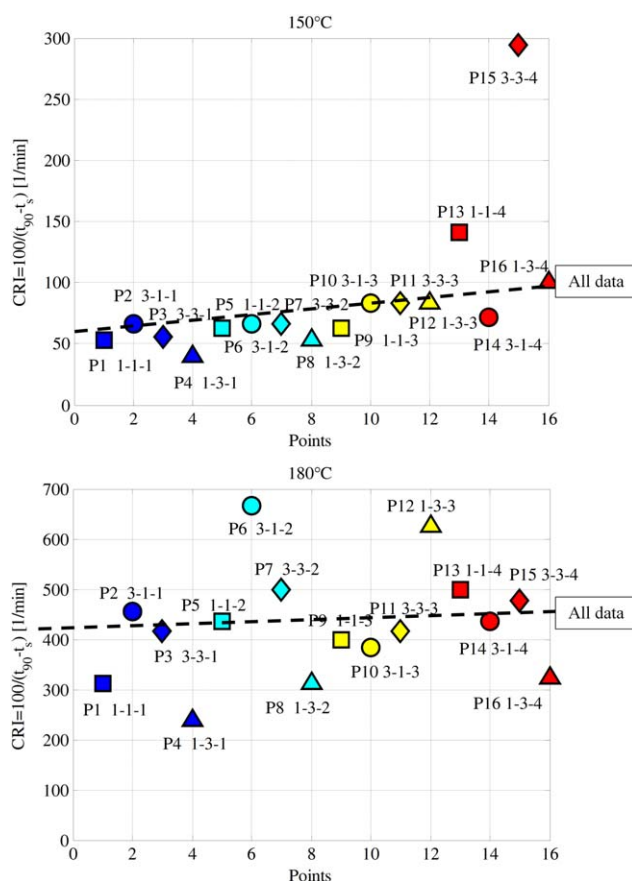
Figure 4. Experimental Cure Rate Index (CRI) at 150 °C (top) and 180 °C (bottom) as a function of S-TBBS-DPG concentration variations. [Color figure can be viewed in the online issue, which is available at wileyonlinelibrary.com.]
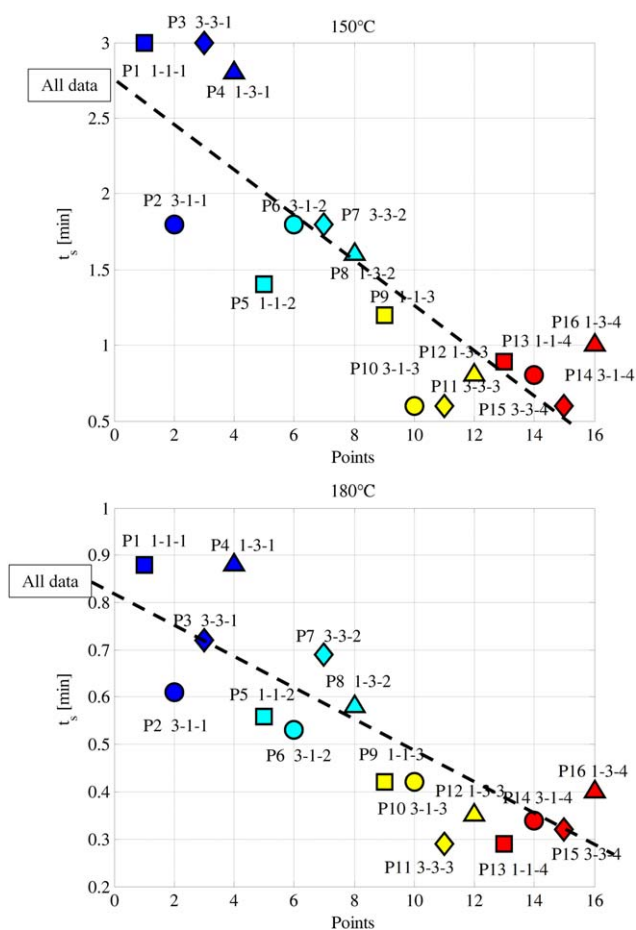
Figure 5. Experimental scorch time (t_s) at 150°C (top) and 180°C (bottom) as a function of S-TBBS-DPG concentration variations. [Color figure can be viewed in the online issue, which is available at wileyonlinelibrary.com.]

Experimental CRI at 150 and 180 °C is represented in Figure 4, whereas scorch time (t_s) in minutes at the same temperatures is depicted in Figure 5. Finally, in Figure 6, $t_{100}-t_s$ again at 150 and 180 °C for all points experimentally investigated is reported. Linear regressions are also represented, showing a substantial independence from S and TBBS concentrations.

From an overall analysis of the results, in general, it can be affirmed that, from a quantitative standpoint, DPG tends also (1) to reduce drastically induction, as illustrated in Figure 5 where t_s is represented for all points experimentally tested and (2) to increase reversion %, see Figure 2. The role played by DPG is consistently kept also by the numerical model adopted in the article, as it will be shown in Discussion and Considerations on the Computed Kinetic Constants section. It is worth noting that the reduction of scorch time (and hence induction) may be in some case not preferable in manufacturing application, because long scorch times are directly proportional to processing safety.

S obviously increases the maximum torque (because it is associated to more transversal links between polymer chains)

and TBBS helps in increasing the crosslinking degree, which macroscopically coincides with the maximum torque. This conclusion is again supported by results in Figure 3, where it can be observed that both at 150 and 180 °C maximum values are reached for rhombs (i.e., for S-TBBS equal to 3-3), then for circles (i.e., for S-TBBS equal to 3-1), hence for triangles (S-TBBS equal to 1-3) and in the end for squares (S-TBBS 1-1).

If Figures 4 and 6 are compared, it is worth noting that the slopes of the linear regressions are positive in Figure 4 and negative in Figure 6. Apparently against intuition, they however have the same physical meaning because, in Figure 4, $t_{90}-t_s$ are at the denominator.

Finally and as expected, lower curing temperatures are associated with higher values of maximum torque.

From a comparative analysis of CRI, $t_{100}-t_s$ and t_s diagrams for each point investigated at both 150 and 180 °C, it is pretty clear how only the concentration of DPG has a drastic effect on the reduction of t_s and a proportional reduction of t_{100} and t_{90}. This notwithstanding the rate of cure, roughly represented by CRI,
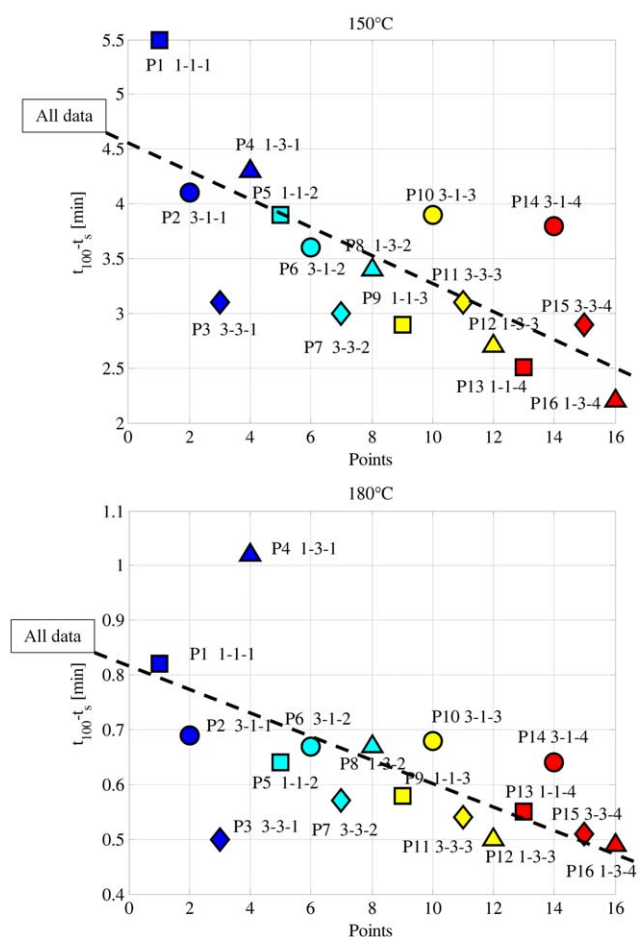
Figure 6. Correlation between ($t_{100}-t_s$) at 150°C (top) and 180°C (bottom) as a function of S-TBBS-DPG concentration variations. [Color figure can be viewed in the online issue, which is available at wileyonlinelibrary.com.]
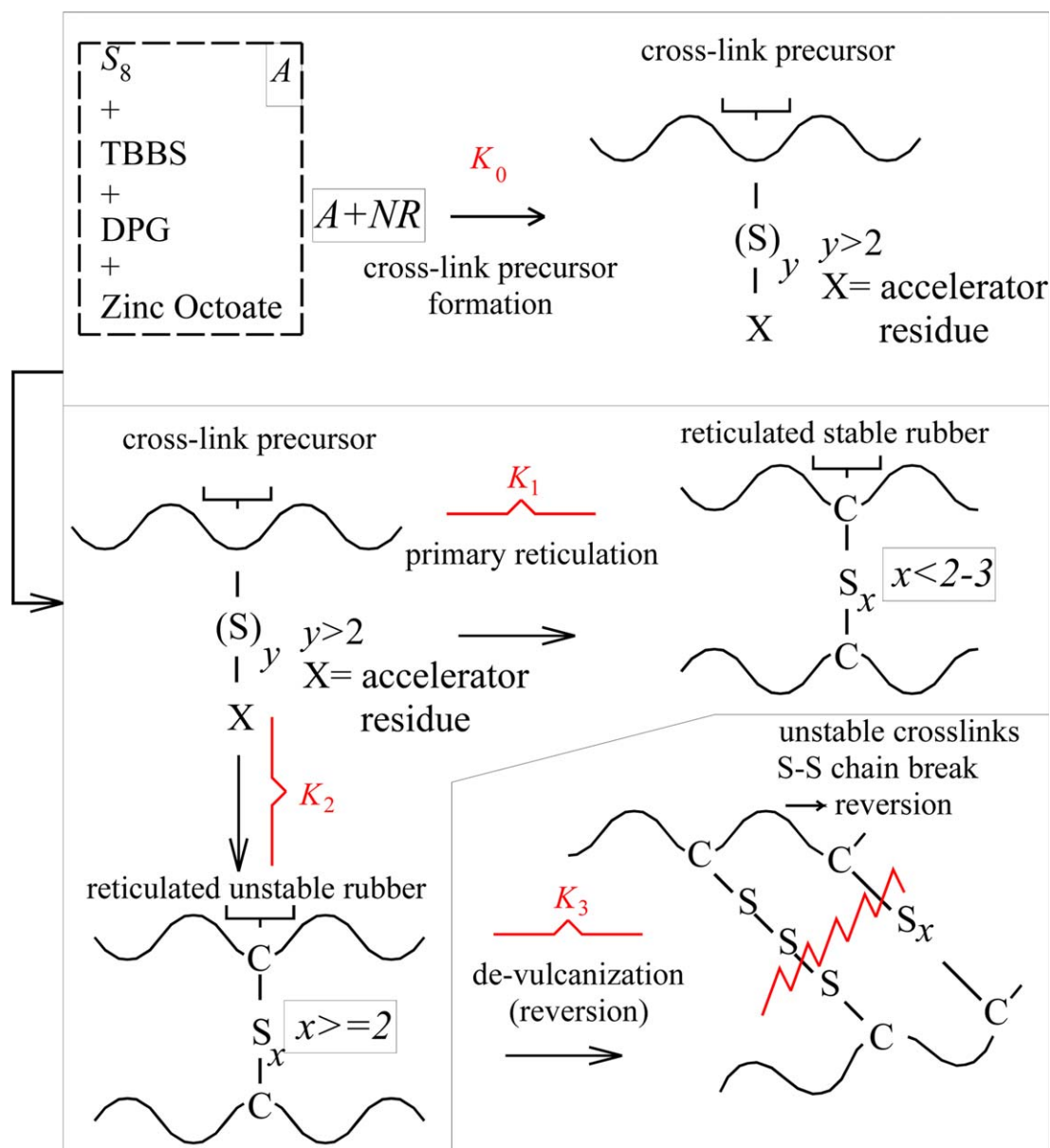
Figure 7. Schematic representation of reactions occurring during NR curing with accelerated sulfur. [Color figure can be viewed in the online issue, which is available at wileyonlinelibrary.com.]

remains almost constant, especially at 150 °C. Therefore, it can be argued that primary vulcanization rate is substantially insensitive to DPG concentration. Cure velocity obviously increases at high temperatures, as demonstrated by the CRI increase, roughly passing from about 80 to 450 min^{-1}, see Figure 4.

THE KINETIC APPROACH PROPOSED

The kinetic approach proposed is extensively presented in its technical details by Milani and co-workers[17,18] where the reader is referred for a comprehensive explanation. We use here a modification of the well-known Han's model for rubber vulcanized with sulfur, that takes into account the contemporary presence of two accelerators with negligible interaction. Before fitting, the numerical model is expected to behave poorly and the optimization strategy adopted is indeed aimed at minimizing the deviation of the numerical rheometer curves from experimental evidences. After optimization, it is expected that numerical curves fit quite well experimental evidences, with interesting implications on practical issues. The basic reaction schemes assumed are classic and refer to existing literature in the field. Such schemes are known from the scientific literature,[5,7,13,15] as mentioned above. A graphic schematization of the reactions occurring is reported in Figure 7 for the sake of clearness.

As known, many reactions occur in series and parallel during NR cured with sulfur. To take into consideration all the chemical
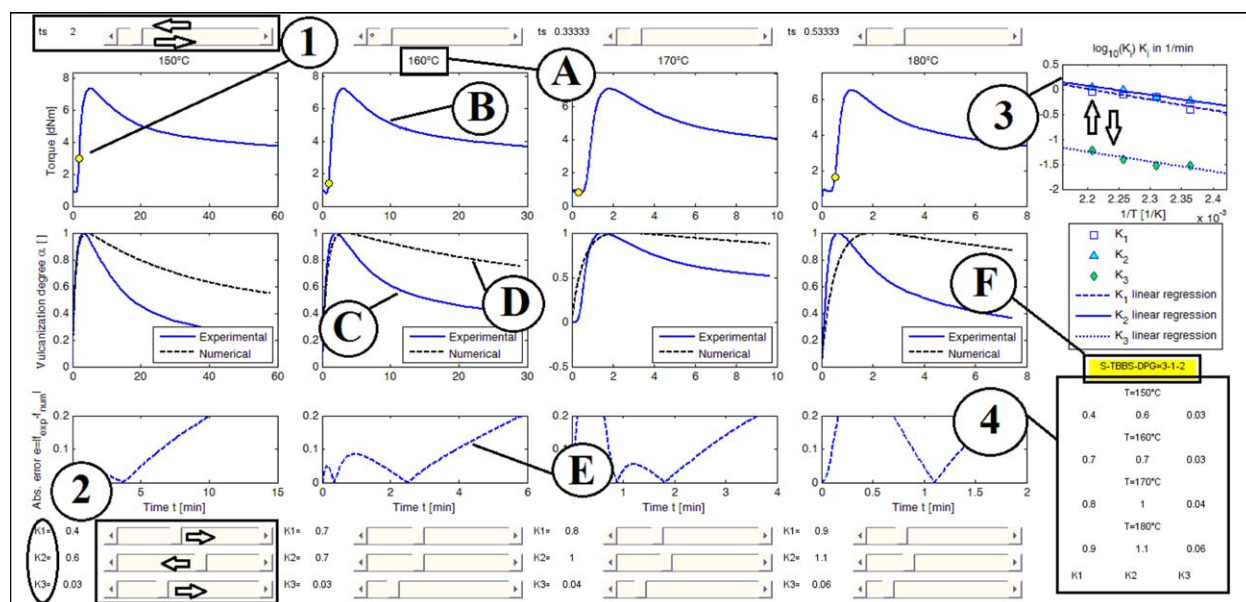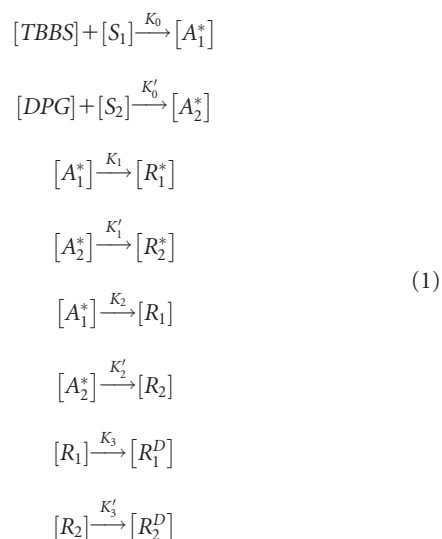
Figure 8. Screenshot of the GUI software used to heuristically optimize the kinetic constants on available experimental data. [Color figure can be viewed in the online issue, which is available at wileyonlinelibrary.com.]

phenomena occurring is not an easy task, but suitable simplified models that fit reasonably well experimental data are already available from Han *et al.*,[15] Leroy *et al.*,[5] and Milani *et al.*[7] Typically, the chain reactions are initiated by the formation of macroradicals or macro-ions representing the intermediate crosslink precursor. This occurs in the so-called induction period, which is usually excluded from computations, being torque more associated to viscosity rather than crosslinking. Such reaction may anyway be associated, from a kinetic theory point of view, to a reaction velocity represented by the kinetic constant K_0.

After induction, the actual cross-linking proceeds roughly through two pathways, which have been shown to be additive, namely the formation of the stable and unstable crosslinked polymer. In the first case, single or double strong S-S bonds link two contiguous polymer chains, whereas unstable crosslinks are usually associated to multiple S-S bonds. In this latter case, crosslinked polymer evolves with high probability to a break of the bond and hence de-vulcanization, which can occur with a backbiting of the bond in the same backbone chain or a simple detachment of the polymer chains. When two accelerators are present, as for instance TBBS and DPG, reactions with each single accelerator occur reasonably in parallel, that is, with negligible interaction between the two agents. There is experimental evidence of little TBBS-DPG interaction[20]; however, the matter is still under study by the authors from a chemical point of view and in any case it can be hardly translated into mathematics. All the reactions considered occur with a kinetic velocity depending on the temperature reaction, associated to each kinetic constant.

Denoting with K_i and K_i' the *i*th kinetic constant associated to TBBS and DPG respectively and with index 1 (2) the concentration of a chemical quantity reacting/formed with TBBS (DPG), the following kinetic scheme is assumed:

$$[TBBS]+[S_1] \xrightarrow{K_0} [A_1^*]$$

$$[DPG]+[S_2] \xrightarrow{K_0'} [A_2^*]$$

$$[A_1^*] \xrightarrow{K_1} [R_1^*]$$

$$[A_2^*] \xrightarrow{K_1'} [R_2^*]$$

$$[A_1^*] \xrightarrow{K_2} [R_1] \qquad (1)$$

$$[A_2^*] \xrightarrow{K_2'} [R_2]$$

$$[R_1] \xrightarrow{K_3} [R_1^D]$$

$$[R_2] \xrightarrow{K_3'} [R_2^D]$$

In eq. (1), $[S_1]$ and $[S_2]$ are sulfur concentrations reacting with TBBS and DPG respectively, $[A_1^*]$ and $[A_2^*]$ the sulfurating agents, $[R_1^*]$ and $[R_2^*]$ the stable crosslinked chain (S-S single bonds), $[R_1]$ and $[R_2]$ the unstable vulcanized polymer, $[R_1^D]$ and $[R_2^D]$ the de-vulcanized polymer fraction (reversion). $K_{0,1,2,3}$ and $K_{0,1,2,3}'$ are kinetic reaction constants. Here it is worth emphasizing that $K_{0,1,2,3}$ and $K_{0,1,2,3}'$ are temperature dependent quantities, hence they rigorously should be indicated as $K_{0,1,2,3}(T)$ and $K_{0,1,2,3}'(T)$, where T is the absolute temperature. In what follows, for the sake of clearness, the temperature dependence will be left out. It is worth remembering here that K_i constants are evaluated at 4 different temperatures by means of best fitting on experimental data, therefore their variability is taken into consideration in the model proposed. It is interesting to see, indeed, if the numerically estimated kinetic constants roughly follow and Arrhenius law, that is, if their logarithmic values
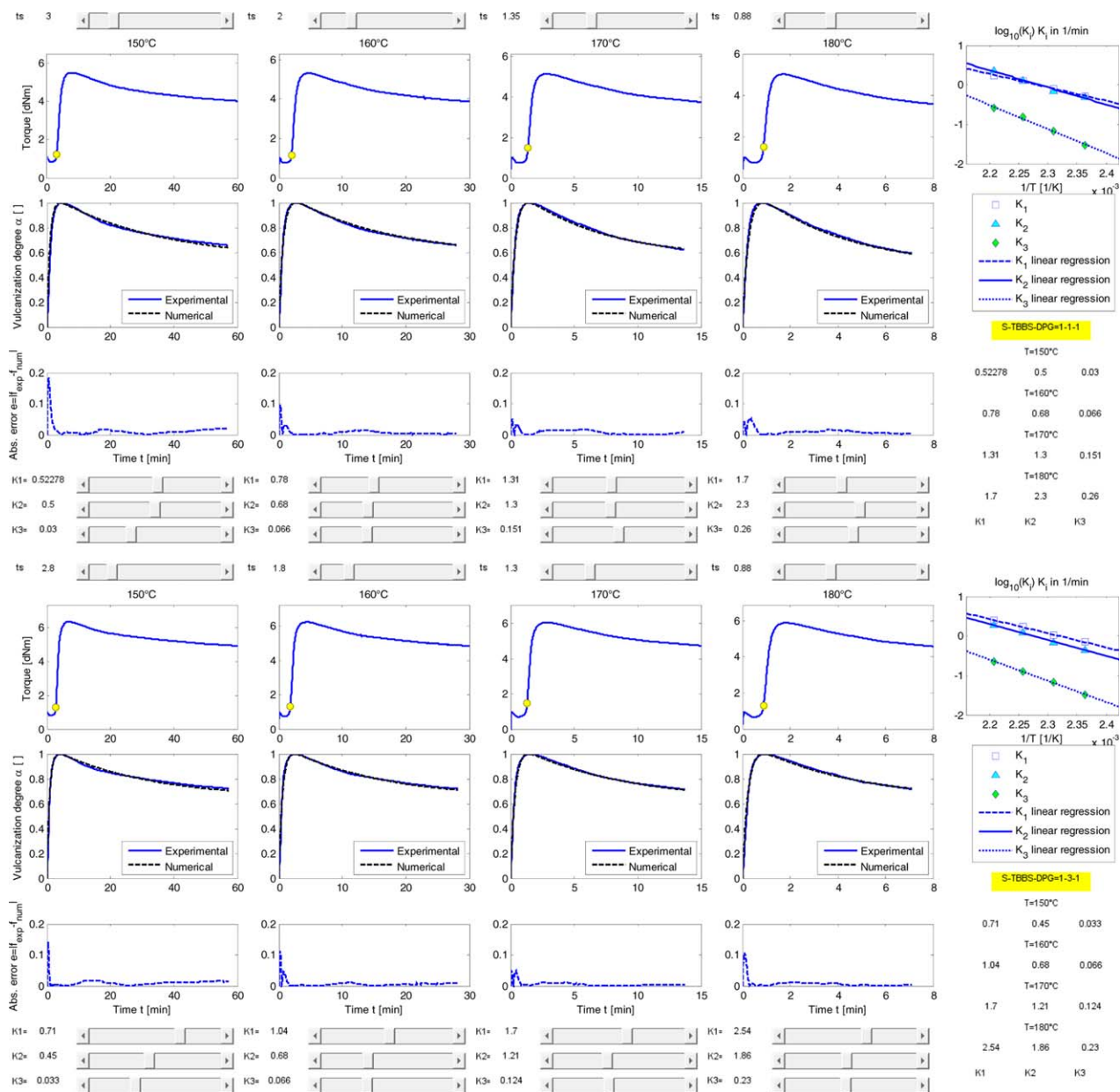
Figure 9. DPG = 1 phr. K_i constants provided by the numerical model. Top: S-TBBS = 1-1 phr. Bottom: S-TBBS = 1-3 phr. [Color figure can be viewed in the online issue, which is available at wileyonlinelibrary.com.]

versus the inverse of the absolute temperature (i.e., on the Arrhenius space) lay approximately on a straight line. Such check is typically an a posteriori demonstration of the suitability of the model proposed.

Furthermore, it can be observed that kinetic constants for such kind of problems are usually expressed in either 1/s or 1/min (in any case 1/time). Since the crosslinking degree typically is

associated to a molar concentration of the polymer, this is usually identified as a reaction velocity. K_0 constant does not obey strictly to a classic kinetic theory, because at the very beginning of the vulcanization process viscosity rules the physical phenomenon instead of chemical reactions.

Excluding K_0, it has been recently shown[17,18] that the crosslinking percentage α admits a closed form solution as follows:

$$
\begin{aligned}
\alpha = r_1 + r_2 = \beta &\left\{ \frac{K_1}{K_1+K_2} \left[1 - e^{-(K_1+K_2)(t-t_i)} \right] + \frac{K_2}{K_1+K_2-K_3} \left[e^{-K_3(t-t_i)} - e^{-(K_1+K_2)(t-t_i)} \right] \right\} \\
+ (1-\beta) &\left\{ \frac{K_1'}{K_1'+K_2'} \left[1 - e^{-(K_1'+K_2')(t-t_i)} \right] + \frac{K_2'}{K_1'+K_2'-K_3'} \left[e^{-K_3'(t-t_i)} - e^{-(K_1'+K_2')(t-t_i)} \right] \right\}
\end{aligned}
\tag{2}
$$
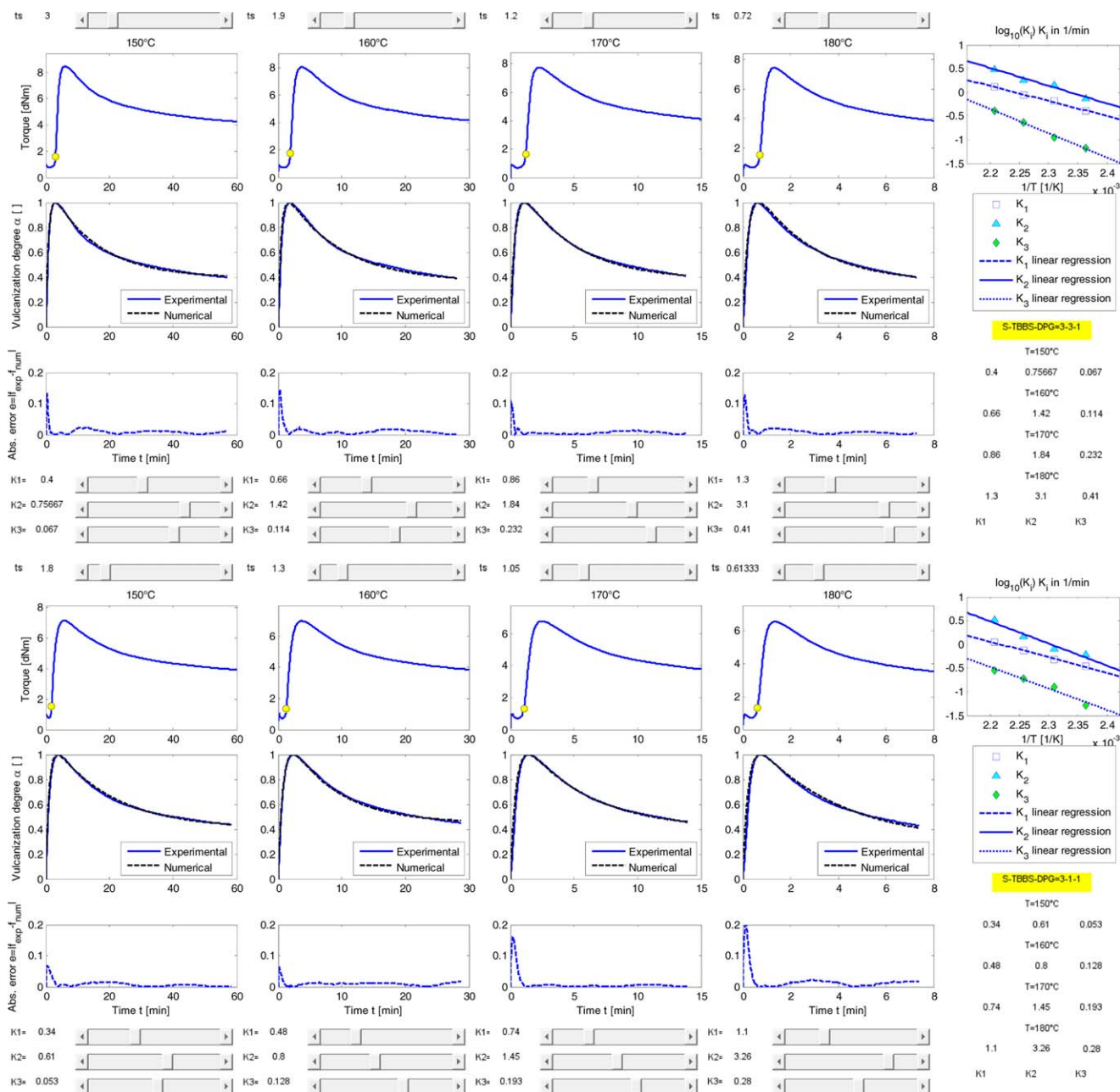
Figure 10. DPG = 1 phr. K_i constants provided by the numerical model. Top: S-TBBS = 3-3 phr. Bottom: S-TBBS = 3-1 phr. [Color figure can be viewed in the online issue, which is available at wileyonlinelibrary.com.]

β is rigorously a parameter ranging from 0 to 1, that could be estimated defined as follows:

$$\beta = \frac{[\text{TBBS}]}{[\text{DPG}] + [\text{TBBS}]} \qquad (3)$$

Hereafter, the simplifying hypothesis $\beta = 1$ is assumed in order to discuss results on only three kinetic constants instead of six. From a practical point of view, this is not restrictive, as shown by Milani and coworkers,[17] where the reader is referred for further details.

A direct evaluation of K_1, K_2 (or $K\prime_1$, $K\prime_2$) constants that needs recursive computations has been recently proposed by Milani and Milani,[18] where the reader is referred to for further details.

Here a different heuristic and interactive approach (called GURU, Graphical User interface for RUbber) based on a GUI implementation of experimental rheometer curves and eq. (2) is adopted. Full details of the heuristic software proposed are provided by Milani and Milani.[22] Here only few details are reported to show how even unexperienced users may achieve accurate results, being the present paper mainly focused on the presentation of the experimental/numerical results obtained by the authors.
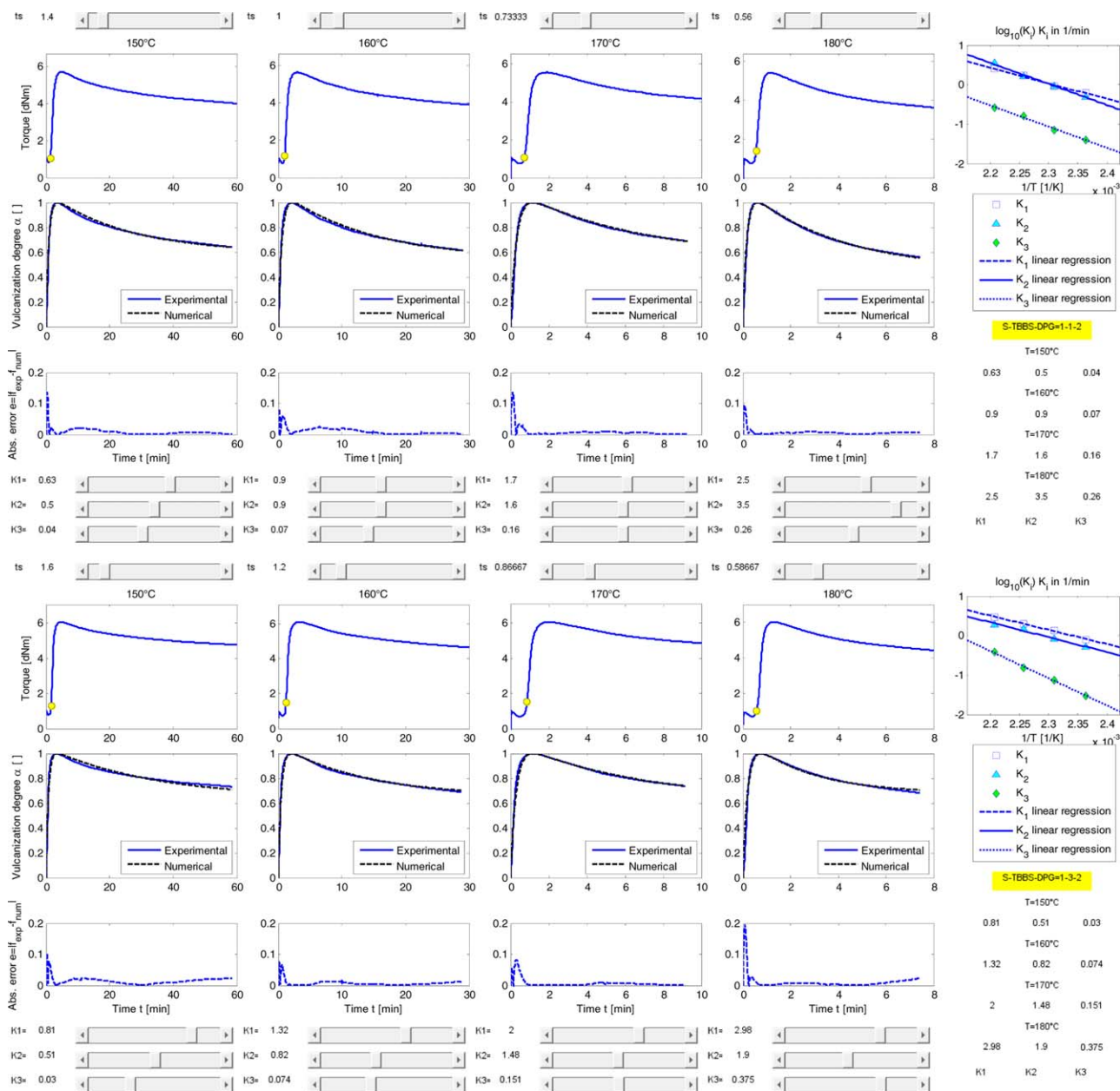
Figure 11. DPG = 2 phr. K_i constants provided by the numerical model. Top: S-TBBS = 1-1 phr. Bottom: S-TBBS = 1-3 phr. [Color figure can be viewed in the online issue, which is available at wileyonlinelibrary.com.]

With reference to Figure 8, where the interface of the software as it appears to the user after having loaded the experimental data to analyze is shown, it can be seen that the output screen-shot has five columns of diagrams.

The first four columns from the left represent synoptically data at a given vulcanization temperature, starting from 150 °C with the column on the left and ending to 180 °C with the fourth column on the right (see detail A in Figure 8).

Each column represents on the top the crude experimental rheometer data (detail B), with an indication of the scorch time adopted (yellow dot moving on the curve after user's action 1 in Figure 8), the performance of the numerical model (detail D) with

respect to normalized experimental curve (detail C) in the central subfigure and the absolute error of the numerical model when compared with normalized experimental curve (detail E).

Kinetic constants are dynamically modified by means of user's action on the sliders on the bottom (action 2). The user can dynamically move the slider by means of a trial and error procedure in order to graphically minimize the absolute difference between experimental and numerical curve. Scorch point can be adjusted as well. Typically the optimization takes few instants. The values of the kinetic constants are dynamically updated and registered in the table situated on the bottom left part of the screen (detail 4) and plotted in the Arrhenius space depicted on the top-left (detail 3). In the same subfigure, the linear regression is also represented.
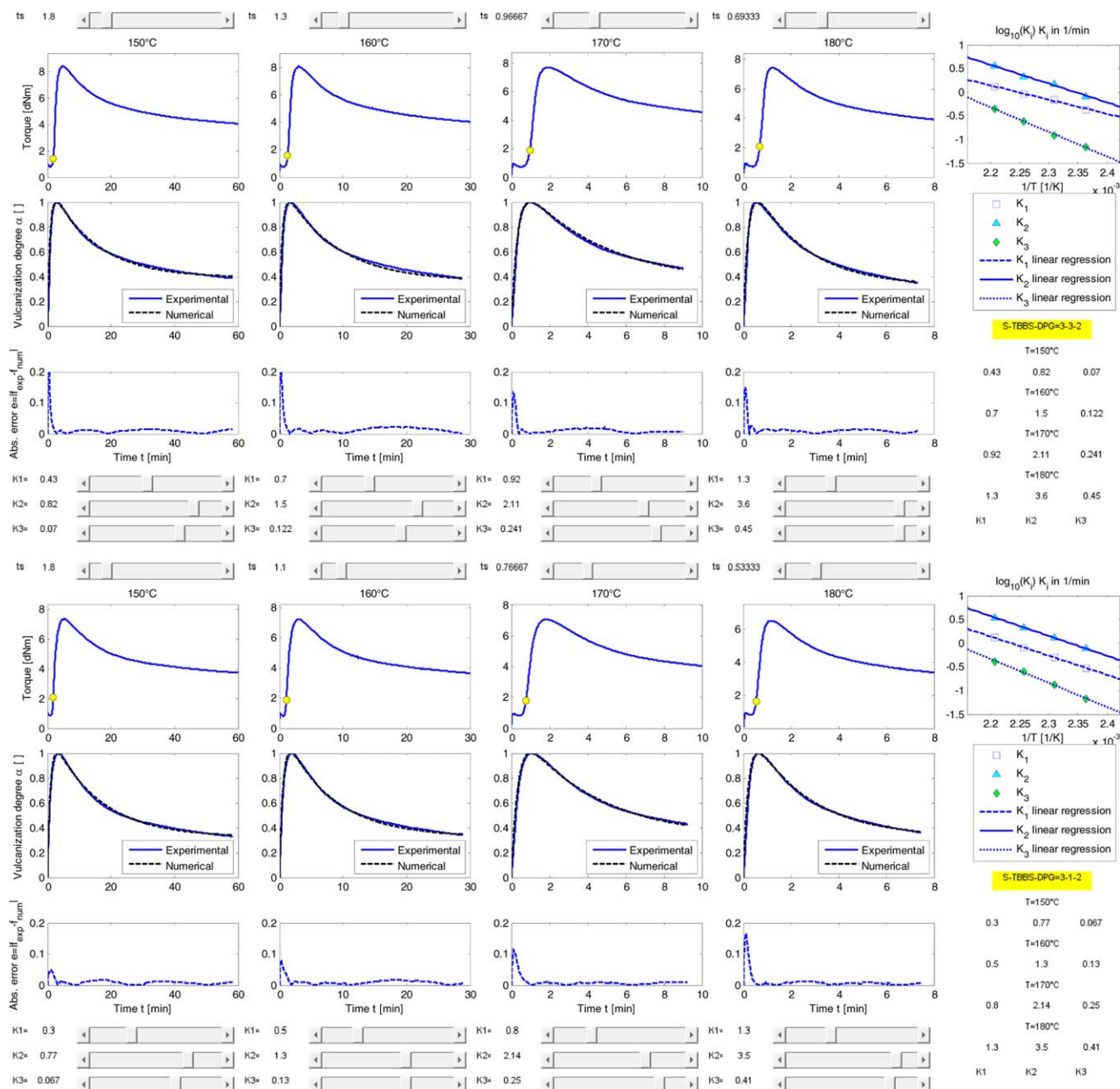
Figure 12. DPG = 2 phr. K_i constants provided by the numerical model. Top: S-TBBS = 3-3 phr. Bottom: S-TBBS = 3-1 phr. [Color figure can be viewed in the online issue, which is available at wileyonlinelibrary.com.]

An indication of the typology of compound analyzed is finally provided in a yellow box (detail F).

As it will be pointed out in the following section by means of a comprehensive comparison of all the numerical data produced, the experimental fitting is almost perfect in the majority of the cases. It is stressed that the determination of the kinetic constants of the rheometer curve investigated is almost immediate, because occurs dynamically without the need of any particular ability by the user and without the need to have at disposal nonlinear programming routines.

NUMERICAL SIMULATIONS

A huge amount of numerical analyses (64) are performed on the experimentally tested compounds of Figure 2, with the aim of deriving the following information:

  i. kinetic constants of the model for each example;
 ii. infer the behavior of the different compounds outside the temperature range inspected;
iii. deduce systematic relations between the values of the constants at different accelerators and sulfur concentrations.
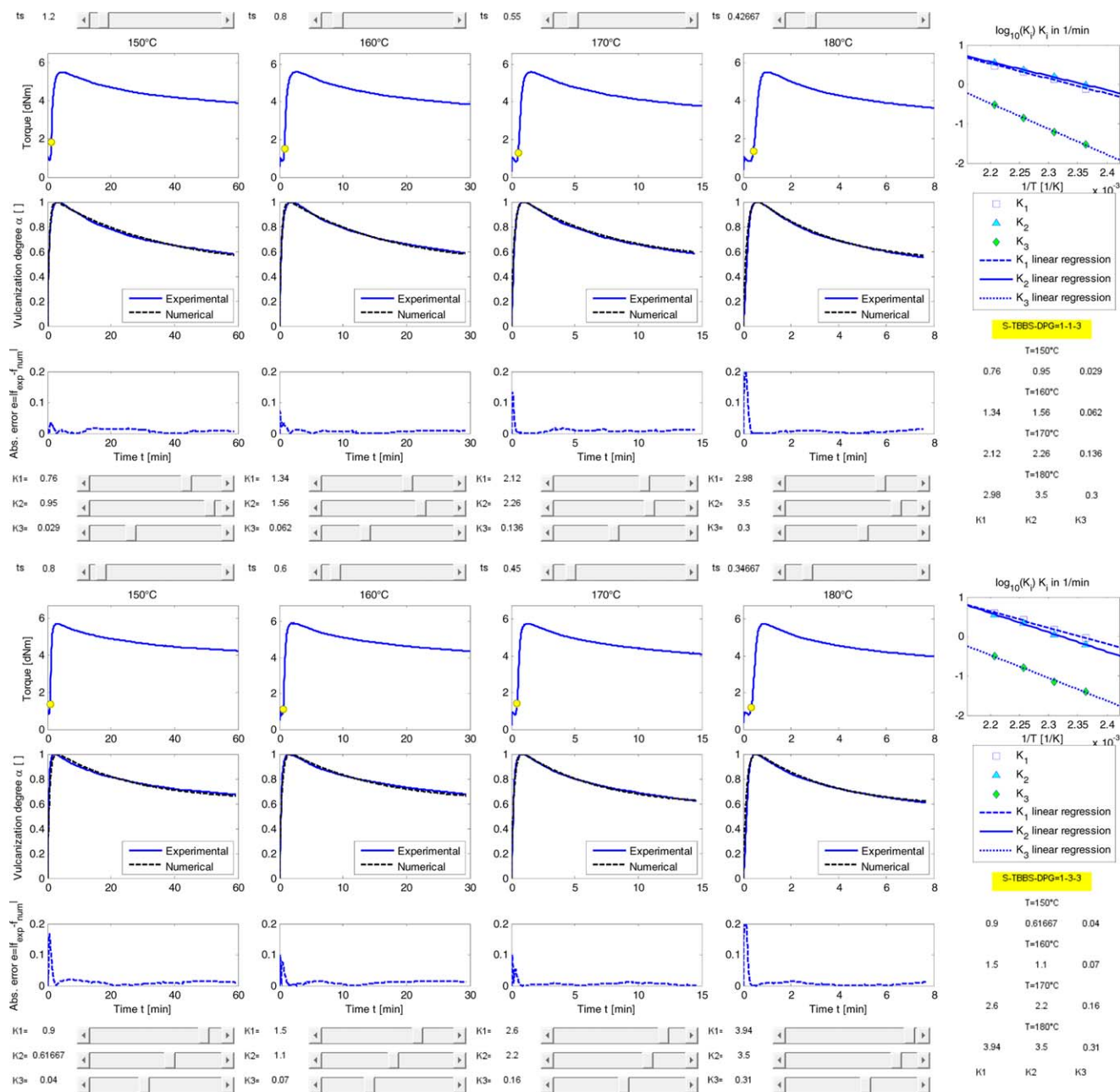
Figure 13. DPG = 3 phr. K_i constants provided by the numerical model. Top: S-TBBS = 1-1 phr. Bottom: S-TBBS = 1-3 phr. [Color figure can be viewed in the online issue, which is available at wileyonlinelibrary.com.]

The experimental reliability of the numerical procedure presented, similarly to the validation done by Milani et al.[7] and Milani and Milani,[8] is tested on a normalized version of the experimental rheometer data. One of the most diffused methods of normalization, which heuristically links the vulcanization degree with experimental rheometer torque is the Sun and Isayev[23] procedure. In such a procedure, the $S'(t)$ torque is used as a measure to calculate the evolution of the vulcanization degree $\alpha_{exp}(t)$ through the following formula:

$$\alpha_{exp}(t) = \frac{S'(t) - S_{\min T}}{S_{\max T_0} - S_{\min T_0}} \quad (4)$$

where $S_{\min T}$ is the minimum value of torque S' during a cure experiment at temperature T (before reaching this minimum

value, α_{exp} is considered equal to zero); $S_{\min T_0}$ and $S_{\max T_0}$ are the minimum and maximum torque values, obtained for a cure experiment at a temperature T_0 low enough to allow neglecting reversion. In other words, the low temperature "reversion free" increase of mechanical properties during cure is taken as a reference, to estimate the influence of reversion at higher temperatures, which results in a final degree of vulcanization lower than 100%.

In the present case, it is noted how from experimental curves, in almost the totality of the cases, the peak torque does not exhibit large variations at the different vulcanization temperatures tested.
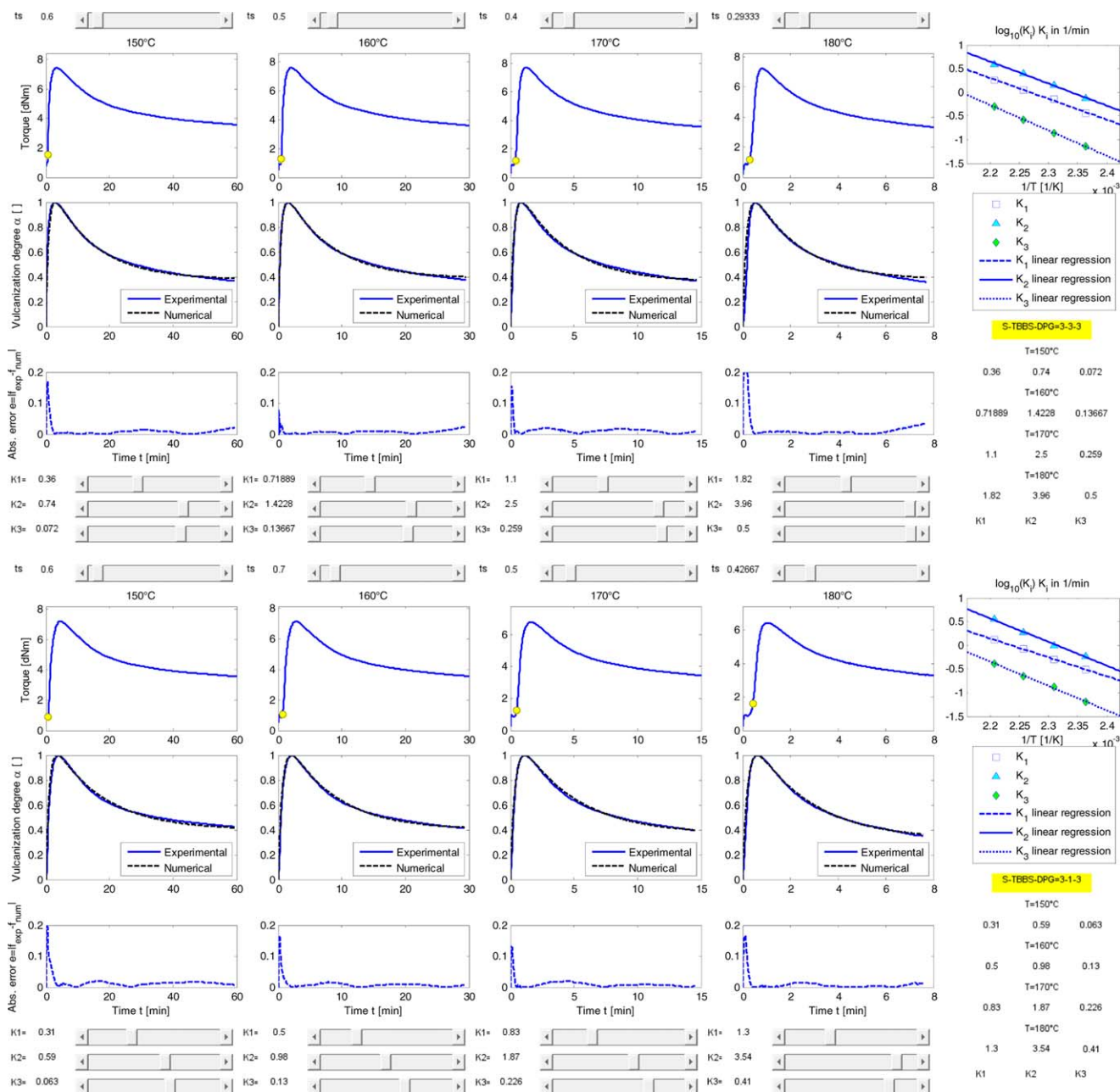
Figure 14. DPG = 3 phr. K_i constants provided by the numerical model. Top: S-TBBS = 3-3 phr. Bottom: S-TBBS = 3-1 phr. [Color figure can be viewed in the online issue, which is available at wileyonlinelibrary.com.]

Therefore a more straightforward but still effective normalization approach could be adopted, which relies into the exclusion from computations of all points before scorch time and into the normalization of the torque values with the maximum torque reached at that temperature. In other words, the following formula for $\alpha_{exp}(t)$ could be utilized:

$$\alpha_{exp}(t) = \frac{S'(t) - S_{\min T}}{S_{\max T} - S_{\min T}} \quad (5)$$

Note that using eq. (5), $\alpha_{exp}(t)$ always ranges between 0 and 1 at each temperature, whereas using eq. (4) it may occur that the maximum value of $\alpha_{exp}(t)$ is slightly lower than 1, especially for high vulcanization temperatures. In GURU eq. (4) is implemented.

In any case, it has been demonstrated by Leroy et al.[5] and Milani et al.[17] that the differences obtained using for the normalization eq. (4) or eq. (5) are negligible from a practical point of view, especially in this particular dataset, as shown by Milani et al.[17]

In figures from Figures 9 to 16, the capability of the model to fit rheometer data is benchmarked on the 16 S, DPG, and TBBS concentrations previously mentioned at all curing temperatures investigated (150, 160, 170, 180 °C). Results are presented starting from Plane I (Points from P1 to P4, see Figure 2) in Figures 9 and 10 and ending with Plane IV (Points from P13 to P16) in Figures 15 and 16. Each figure contains two datasets. For
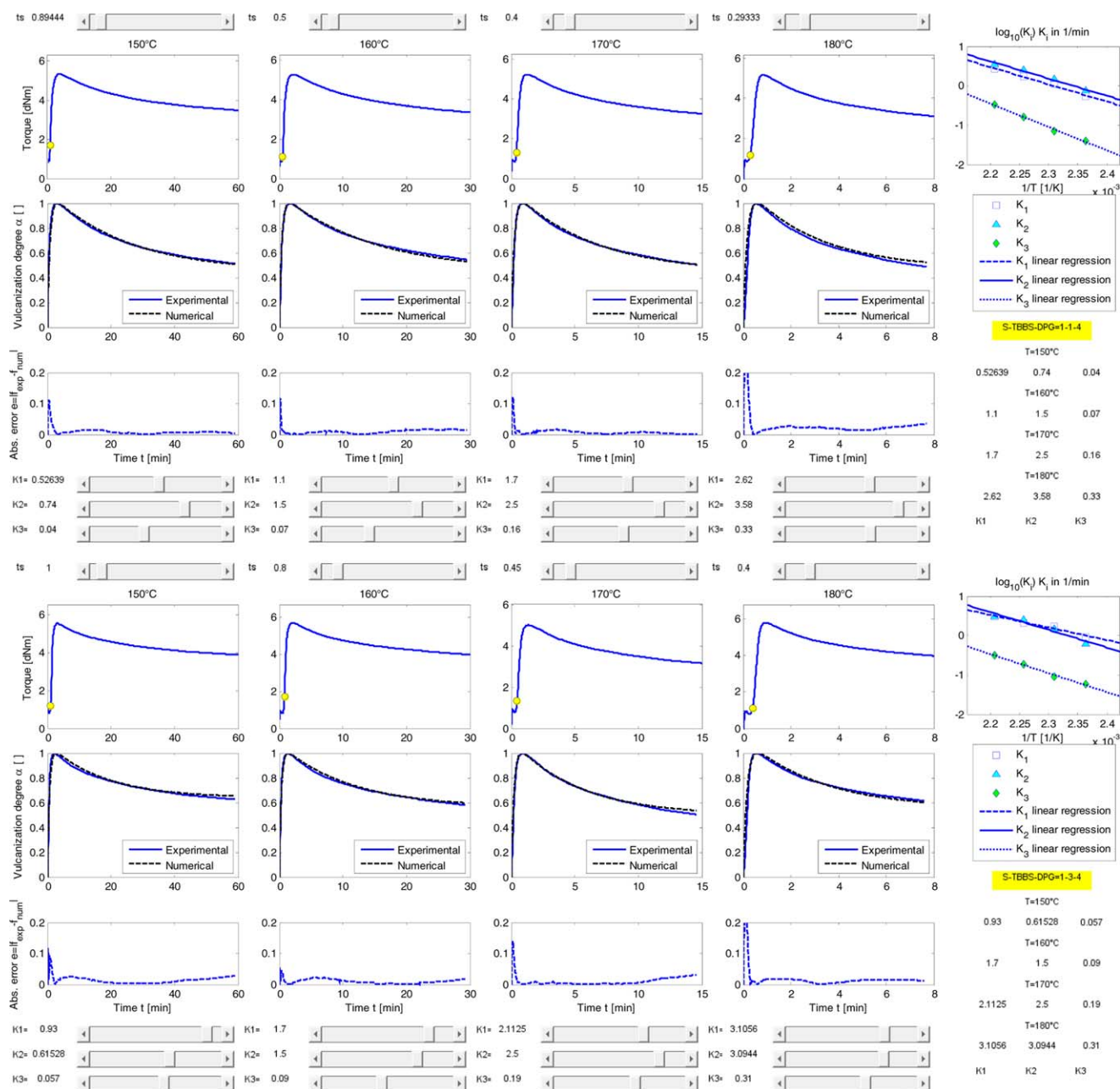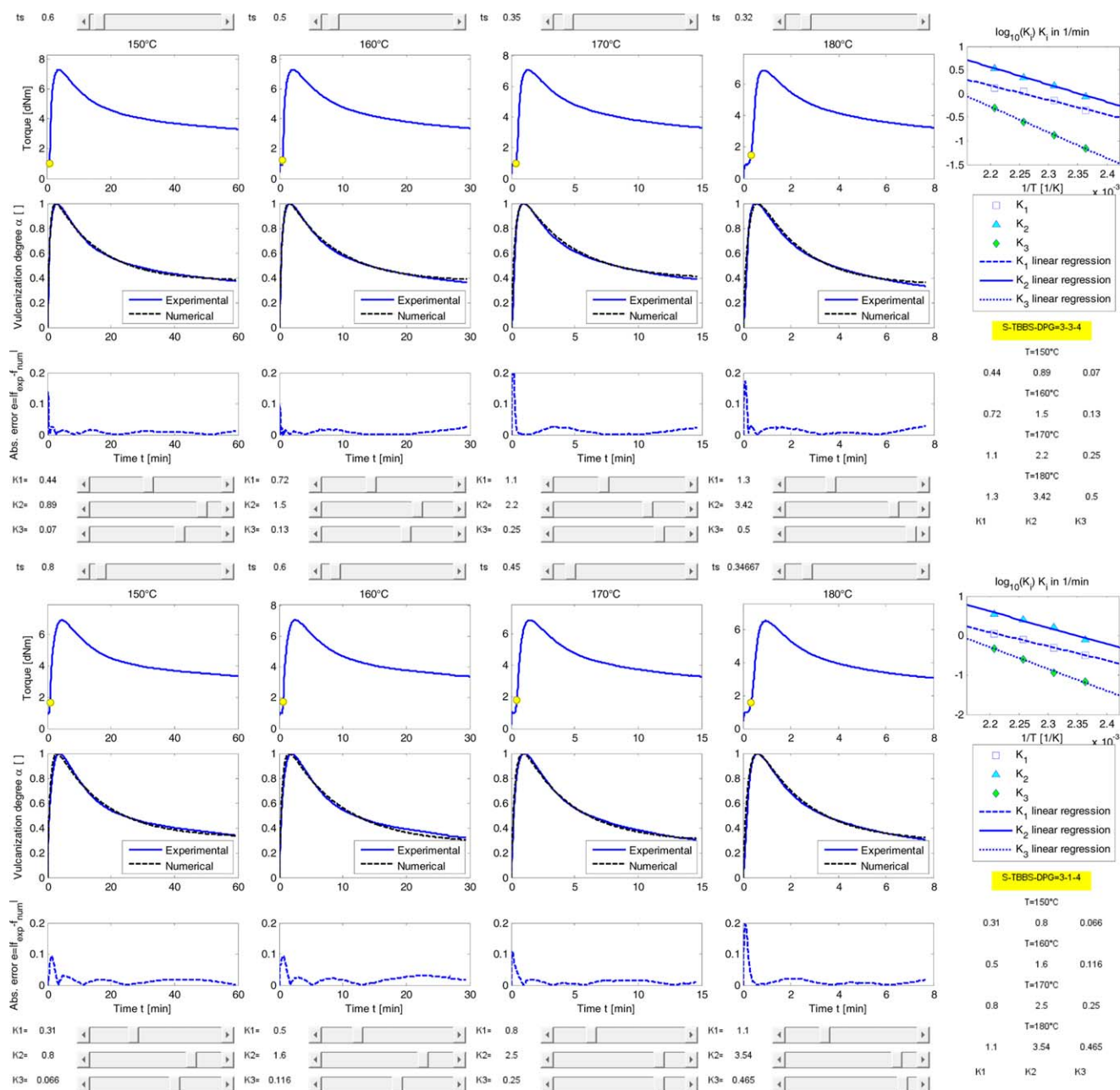
Figure 15. DPG = 4 phr. K_i constants provided by the numerical model. Top: S-TBBS = 1-1 phr. Bottom: S-TBBS = 1-3 phr. [Color figure can be viewed in the online issue, which is available at wileyonlinelibrary.com.]

instance Figure 9 represents the performance of the numerical model at DPG = 1 and with S-TBBS concentrations equal to 1-1 (top sub-figure) and 1-3 (bottom sub-figure).

It has to be emphasized that the GUI model proposed evaluates constants K_1–K_3 (not K_0 which is excluded according to Han's theory because associated to pre-vulcanization, that is, to viscous phenomena) by means of eq. (2). Such numerical estimation occurs finding K_1–K_3 that interactively (moving the associated sliders into GURU interface) allow for the optimal numerical approximation of experimental rheometer curves. The only difference between present GUI approach and other procedures already presented in the technical literature is that

here we use an interactive strategy, that is, the user simply moves some sliders to optimize the numerical curves, whereas the standard way of proceeding is the utilization of least-squares nonlinear optimization algorithms. In the last case, unexperienced technicians cannot estimate easily kinetic constants, whereas the present approach is suited also for all those practitioners without specialized knowledge on operational research.

From a numerical point of view, one could argue if the GUI interactive approach here proposed provides results that are superimposable with a rigorous numerical technique based on the evaluation of kinetic constants fitting normalized experimental data by means of non-linear least squares. Authors

Figure 16. DPG = 4 phr. K_i constants provided by the numerical model. Top: S-TBBS = 3-3 phr. Bottom: S-TBBS = 3-1 phr. [Color figure can be viewed in the online issue, which is available at wileyonlinelibrary.com.]

experienced, for all the cases investigated in the paper, an excellent fitting of the normalized experimental rheometer curves and an almost perfect agreement with the output furnished by least squares best fitting, as shown in Figure 17, where a comparison at 150 and 180 °C between K_i constants evaluated with GURU and least squares interpolation is provided for S-TBBS-DPG = 3-1-1.

DISCUSSION AND CONSIDERATIONS ON THE COMPUTED KINETIC CONSTANTS

Experimental data at disposal, as already pointed out, are at four increasing curing temperatures (namely 150, 160, 170, and

180 °C) for all the S-TBBS-DPG concentrations investigated. Thanks to such superabundant set of simulations at different temperatures, it is interesting to check if the kinetic constants found by means of the proposed numerical approach follow—at least in an approximate way—a linear behavior in the Arrhenius space, that is, where the horizontal axis is represented by the inverse of the absolute curing temperature and the vertical axis is the logarithm of the kinetic constant.

Results for concentrations P1-P4, P5-P8, P9-P12, and P13-P16 are depicted, respectively, in Figures 18, 19, 20 and 21. The lines represented in each figure are obtained by linear regression of the four numerical values of the constants coming from the
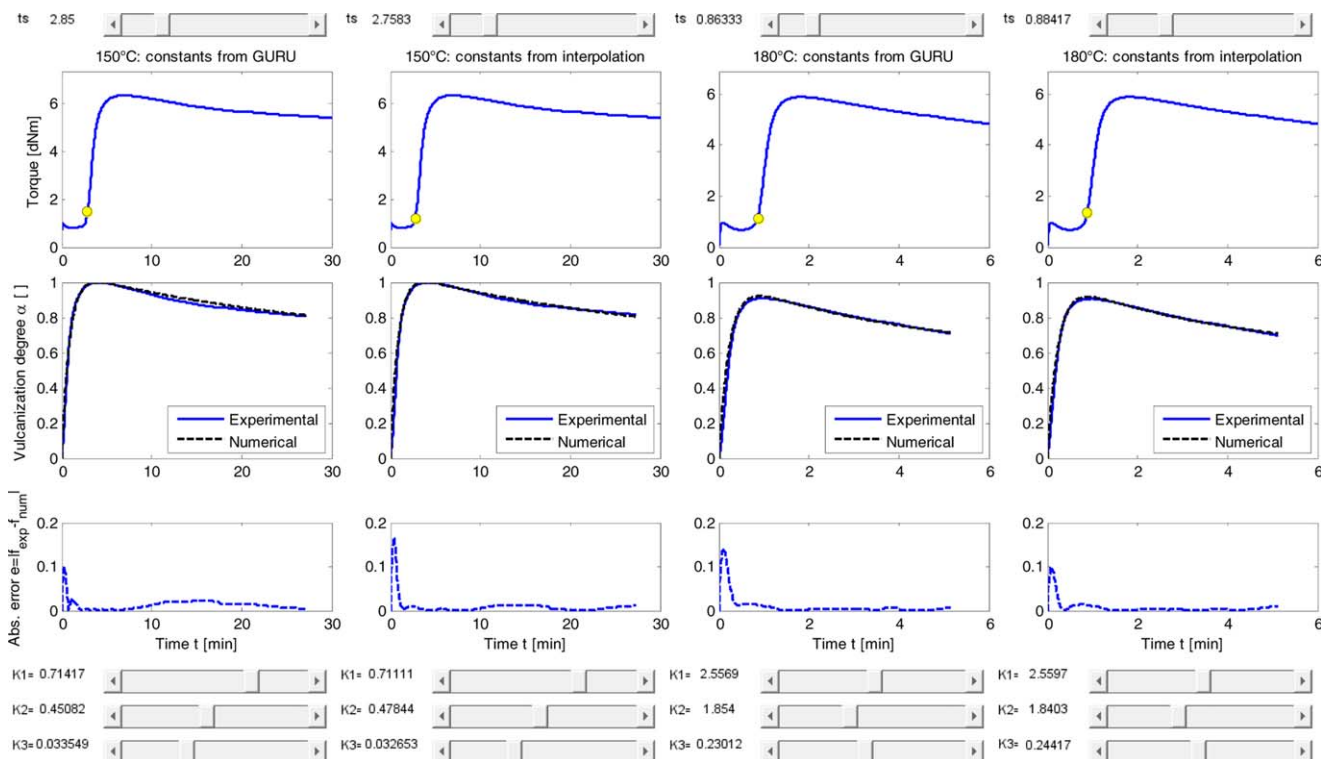
Figure 17. Comparison at 150 and 180°C between numerical and normalized experimental data for S-TBBS-DPG = 3-1-1 obtained by GURU and least squares interpolation. [Color figure can be viewed in the online issue, which is available at wileyonlinelibrary.com.]
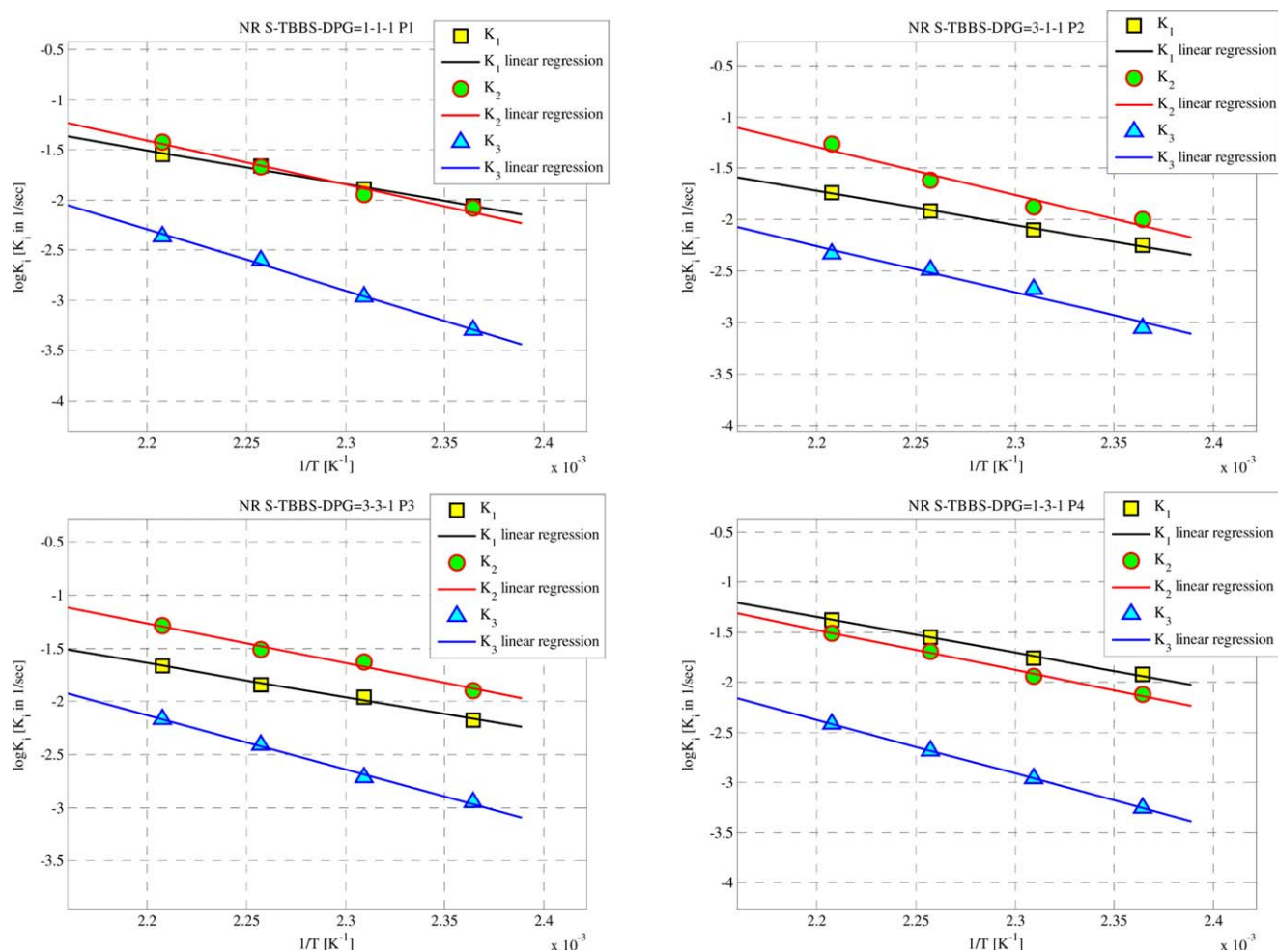

Figure 18. P1-P4 points. K_i constants and related linear regressions according to Arrhenius law at different absolute temperatures in the Arrhenius space. [Color figure can be viewed in the online issue, which is available at wileyonlinelibrary.com.]
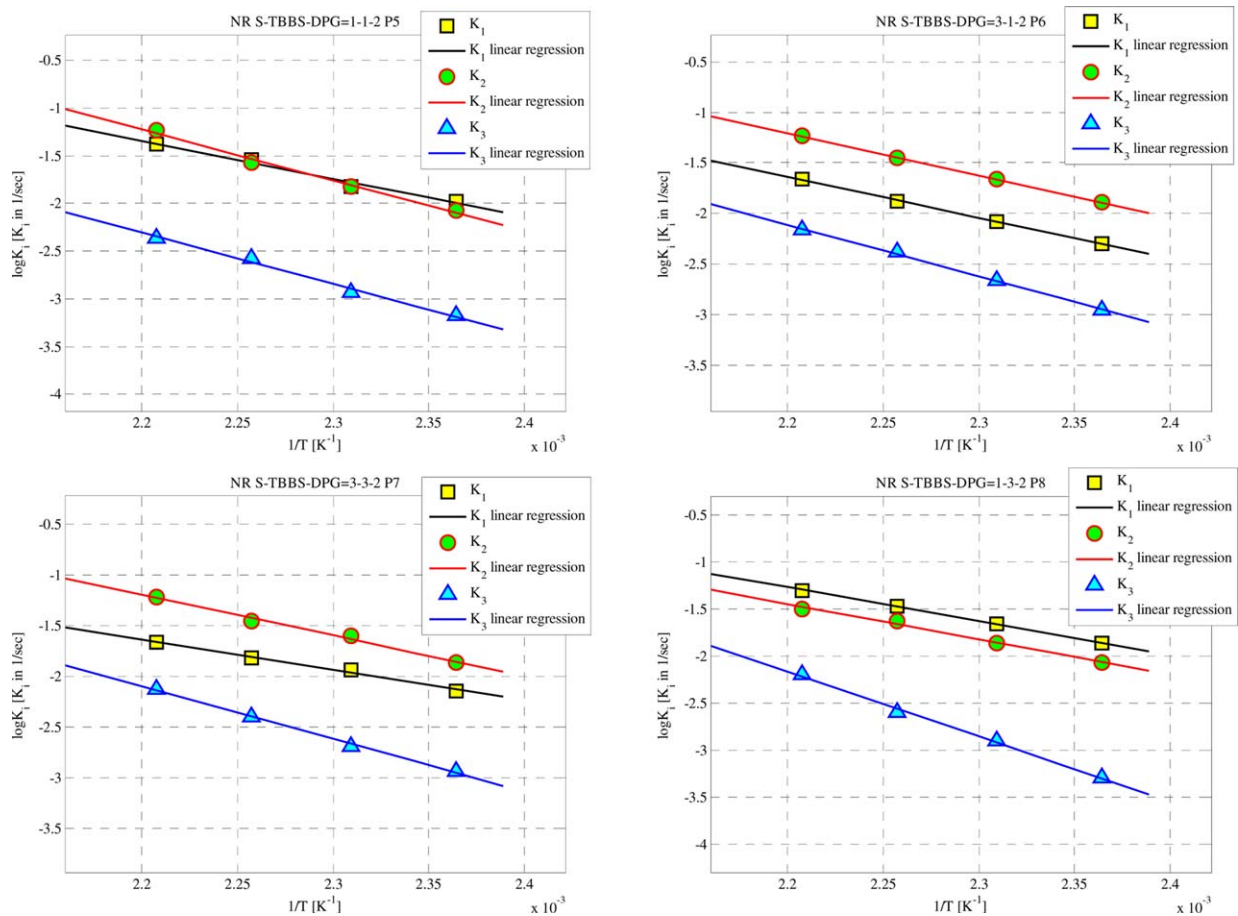
Figure 19. P5-P8 points. K_i constants and related linear regressions according to Arrhenius law at different absolute temperatures in the Arrhenius space. [Color figure can be viewed in the online issue, which is available at wileyonlinelibrary.com.]

Figure 20. P9-P12 points. K_i constants and related linear regressions according to Arrhenius law at different absolute temperatures in the Arrhenius space. [Color figure can be viewed in the online issue, which is available at wileyonlinelibrary.com.]
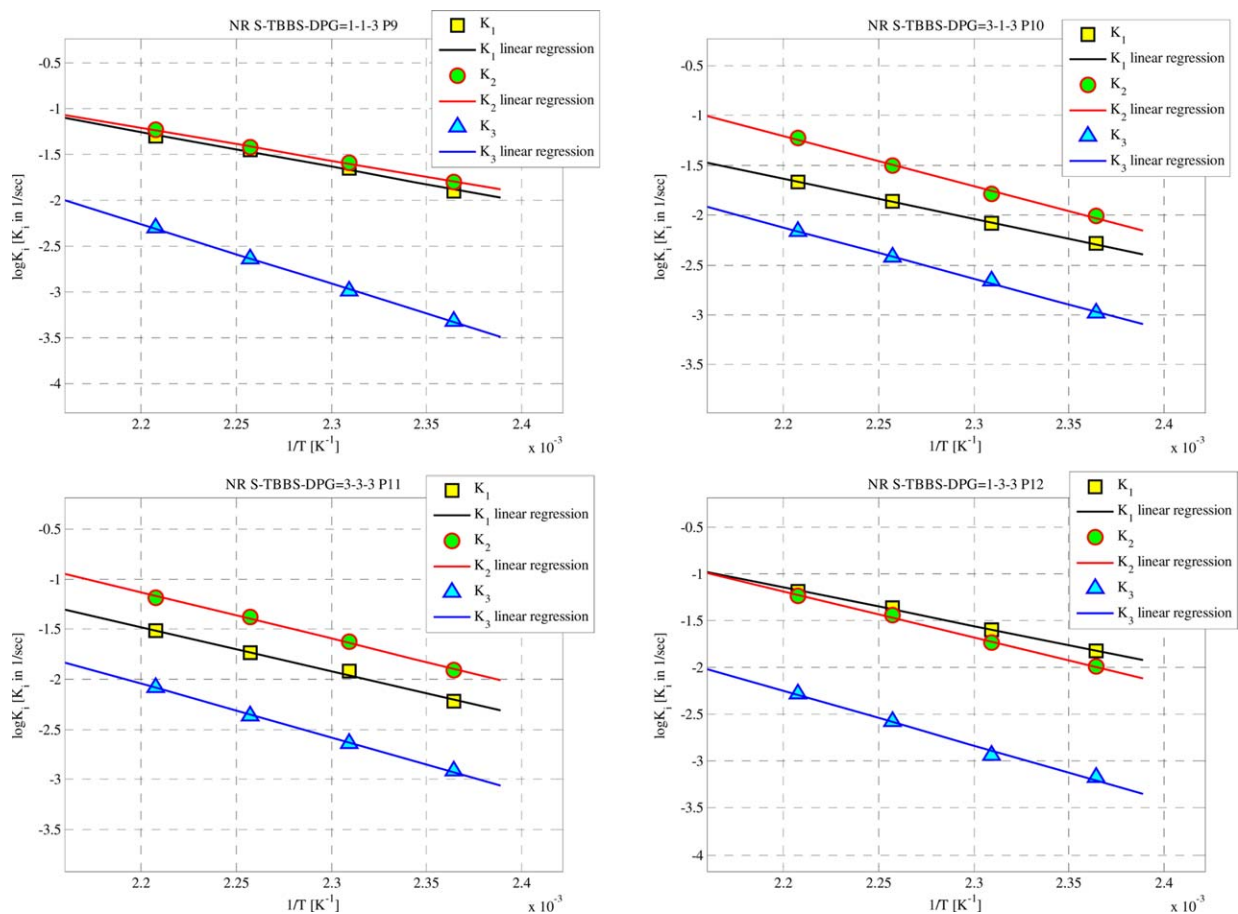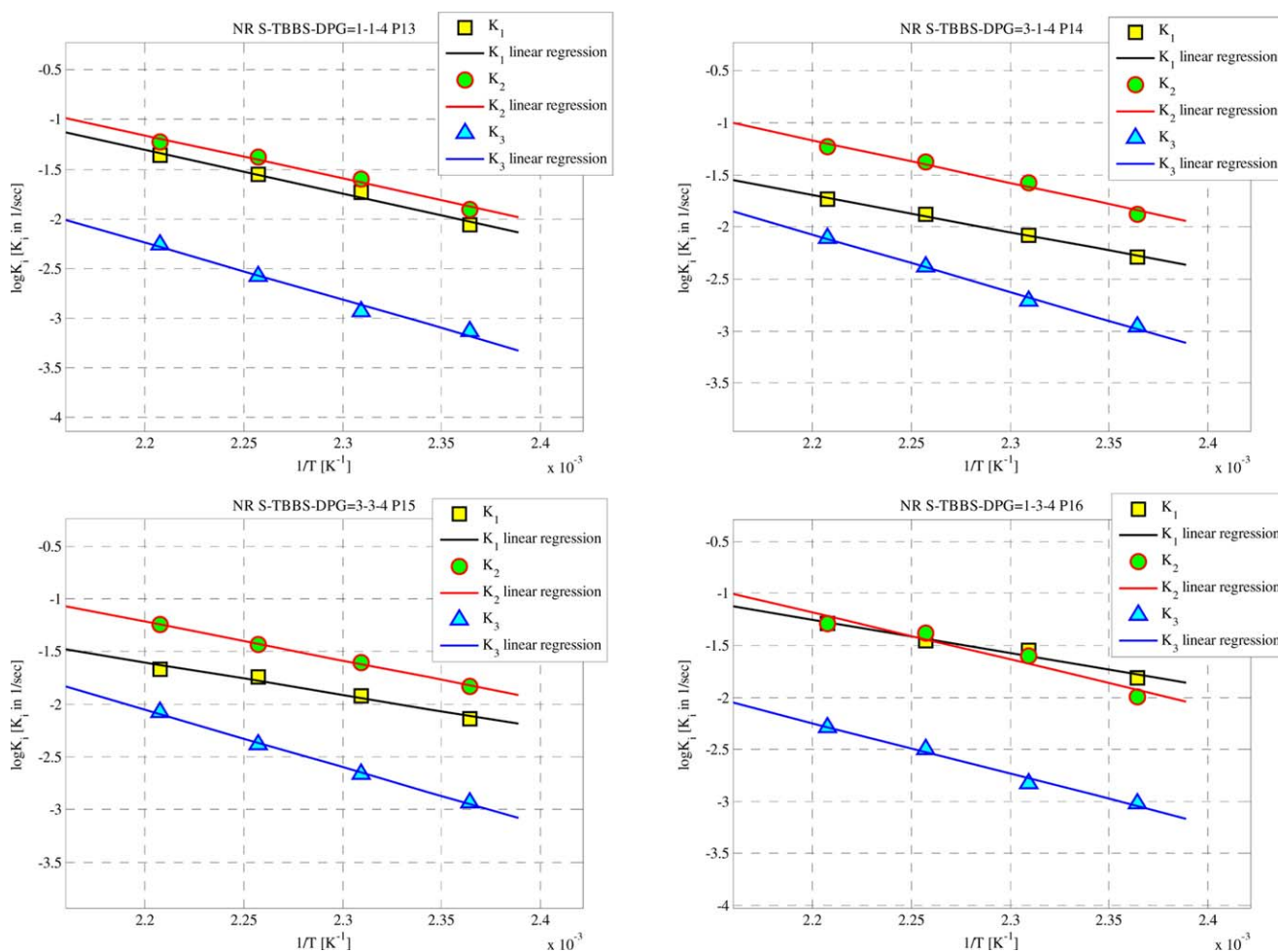
Figure 21. P13-P16 points. K_i constants and related linear regressions according to Arrhenius law at different absolute temperatures in the Arrhenius space. [Color figure can be viewed in the online issue, which is available at wileyonlinelibrary.com.]

proposed fitting at different temperatures. The linear regression determination has the twofold advantage of: (1) providing the activation energy of the kinetic constants and, directly from the figure, (2) to show if the values found for K_i with the numerical procedure at the different temperatures follow the Arrhenius law, that is, a first order temperature dependence of the reaction rates exists.

As can be systematically noted, for all constants, it appears that the trend is acceptably linear, confirming the robustness of the proposed model.

Considering the influences of the three components (S, TBBS, DPG) in relation to the values of the three kinetic constants K_1, K_2, K_3 in the temperature range of experimented data inspected, some further considerations can be done.

In Figure 22, $\log(K_1)$ provided by the kinetic model for P1-P16 points is represented at 150 °C and 180 °C, with the same meaning of the symbols utilized in Figures 2–6. K_1 constants are expressed in s^{-1}. As can be noted K_1 values at both low and high vulcanization temperature (150 and 180 °C) are not very different for all compositions, meaning that the curing rate (or analogously CRI) does not change

considerably adding DPG, as also confirmed by experimentation, see Figure 4.

It is observed how higher K_1s are obtained increasing the TBBS concentration (keeping S concentration constant), both at 150 and 180 °C. As a matter of fact, indeed, 3-3-x and 1-3-x linear regressions are parallel (but associated to higher values) to 3-1-x and 1-1-x ones, respectively.

Within the numerical model K_1 is associated to stable S-S bonds; therefore, it can be argued that TBBS helps in the formation of stable transversal crosslinks.

The role played by DPG is also quite clear, influencing slightly the formation of stable crosslinks when S concentration is small (the slope of the linear regressions for 1-1-x and 1-3-x is indeed small) and appearing much more relevant for a higher concentration of sulfur (with an associated slope of the linear regressions for 3-1-x and 3-3-x quite marked).

Finally (and as expected), an increase of S concentration tends to be responsible for the formation of unstable crosslinks, being therefore associated to lower values of K_1 constants.
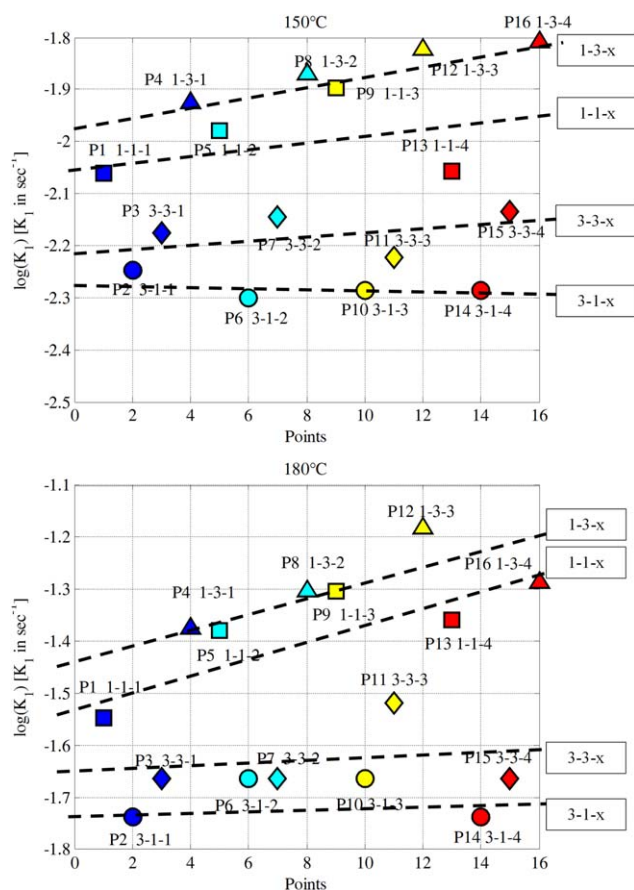
Figure 22. Numerical log(K_1) at 150 °C (top) and 180 °C (bottom) as a function of S-TBBS-DPG concentration variations. [Color figure can be viewed in the online issue, which is available at wileyonlinelibrary.com.]

The evaluation of the role played by K_2 is not an easy task, because it is linked in a nontrivial way to both K_1 and K_3 by means of reactions occurring in series (K_3) and parallel (K_1).

Generally, it has been found that S, TBBS and DPG variation of concentrations results into a change of the evaluated K_2 quite irregular. However, it has been observed that K_i values coming from the numerical model appear roughly in the following linear relation: $K_1 + K_3 = K_2$, as illustrated in Figure 23. Such semiempirical relation may be useful for an indirect estimation of K_2, which is mainly responsible for unstable crosslinks in the model, and hence indirectly to reversion.

It is found that K_2 numerical values are, in general, of the same order of magnitude of K_1 ones; especially for (1,3,1) composition the two reactions, the first forming stable S-S bonds and the second the unstable vulcanized polymer, occur with about the same rate. Such evidence probably suggests that the ratio among the components in relation with S amount is important and has a kinetic effect.

In Figure 24, log(K_3) by the numerical model for P1-P16 points is represented at 150 °C and 180 °C. Again, K_3 constants are expressed in s^{-1}. As can be observed, K_3 is almost independent from TBBS concentration (3-3-x and 3-1-x linear regressions are

almost superimposable at low and high temperatures, the same applies for 1-3-x and 1-1-x lines), obviously it is strongly dependent on S (S = 3 phr is associated to higher values of K_3), but it increases also at high DPG concentrations, especially for S = 1 phr. Being K_3 the numerical counterpart of the reversion %, it can be argued that DPG tends to increase reversion.

K_3 values, in agreement with intuition, are small at low temperature and increase increasing the vulcanization temperatures. The largest values are obtained in the case of the compound (3,3,4). In (3,1,4) compound, where S and DPG concentrations are maximized, the reversion rate drastically increases at high vulcanization temperatures, with a smaller increase of K_1 and K_2 values and lower maximum torque.

In Figure 25, the experimental reversion percentage versus log(K_3) is depicted for points at low (P1-P4-P5-P8-P9-P12-P13-P16) and high (P2-P3-P6-P7-P10-P11-P14-P15) S concentrations, with a linear regression representing the numerical expected behavior, respectively, at 180 and 150 °C in subfigures –a and –b.

From a careful analysis of Figure 25, it is worth noting that both K_3 and reversion % turn out to depend on the curing temperature. In particular, at 150° values found for K_3 (logK_3 ranging from −3.4 to −2.9) are quite lower than those found at 180° (logK_3 ranging from −2.45 to −2.05).
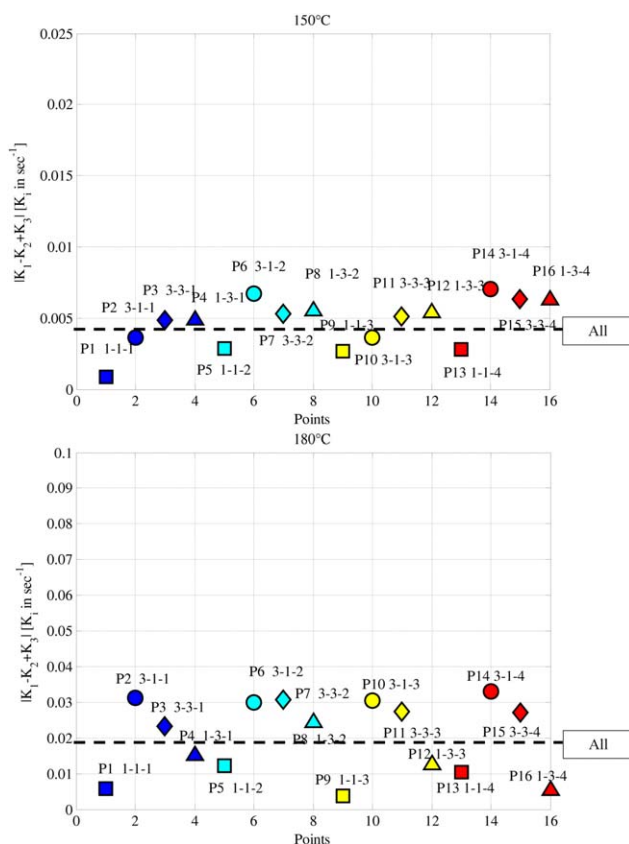
Figure 23. Numerical |K_1−K_2 + K_3| at 150 °C (top) and 180 °C (bottom) as a function of S-TBBS-DPG concentration variations. [Color figure can be viewed in the online issue, which is available at wileyonlinelibrary.com.]
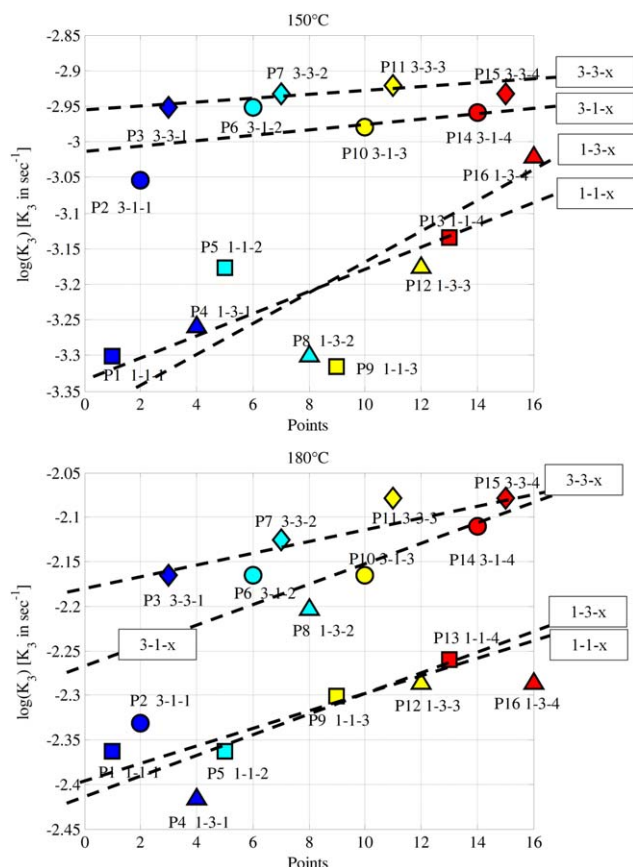
Figure 24. Numerical $\log(K_3)$ at 150 °C (top) and 180 °C (bottom) as a function of S-TBBS-DPG concentration variations. [Color figure can be viewed in the online issue, which is available at wileyonlinelibrary.com.]

The role played by DPG is also quite clear from the figure, where it is shown that, for an increase of DPG concentration (i.e., for points with colors red and yellow), the reversion is generally higher, for both 150 and 180 °C. Figure 25 also shows that reversion experimentally increases with curing temperature.

Such conclusion, demonstrated by the present experimental and numerical results, is in agreement with the undemonstrated statement provided by Akima and Ashim.[24]

CONCLUSIONS

The study carried out is the result of a cooperation between academy (Technical University of Milan) and industry (Pirelli Tyre) on a particular vulcanization system adopted to understand the influence of two accelerators without reinforcing filler.

The investigation was performed combining an experimental and numerical kinetic characterization of a Natural Rubber row material, vulcanized with sulfur, TBBS, and DPG.

Starting from previous kinetic theoretical models by the authors, allowing for a closed form determination of kinetic constants by means of a modification of the Han's model in presence of more than one accelerator, here kinetic constants

are determined changing the concentrations of the three components in a wide range at four temperatures (150, 160, 170, and 180 °C).

Starting from the assumption demonstrated in a companying paper[20] that the interaction between TBBS and DPG may be considered negligible and in any case not quantitatively determinable, the numerical model proposed allows an estimation of the kinetic constants of reaction by means of an interactive heuristic simple approach based on graphical user interface GUI technology.

The mathematical model, whose core is indeed the GUI interface directly utilizable by any practitioner even not expert in the field, exhibited excellent predictive capabilities for the present specific application, but can be easily adapted to any practical case and different curing systems, crosslinking agents as well as accelerators, once that it is put at disposal as freeware software to the scientific community.

From the combined analysis of numerical and experimental results, it is possible to deduce the following considerations:

i. As expected, for all concentrations experimentally tested, values of the kinetic constants K_1, K_2 and K_3 provided by the numerical model increase increasing the vulcanization temperature;
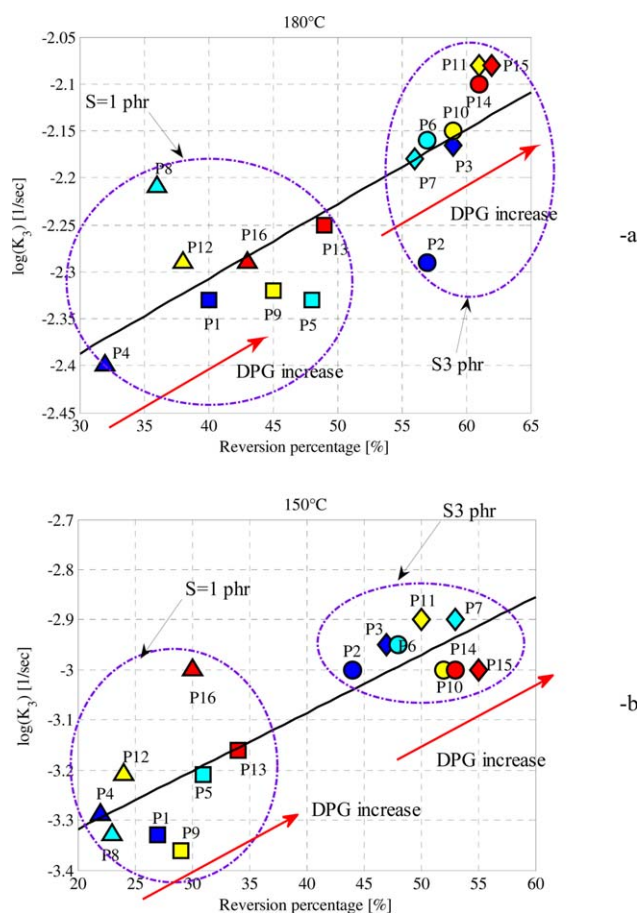
Figure 25. Experimental reversion % versus numerical $\log(K_3)$ for points at zero (P1-P2-P3-P4), low (P5-P6-P7-P8) and high (P9-P10-P11-P12) DPG concentration. (–a) 180 °C; (–b) 150 °C. [Color figure can be viewed in the online issue, which is available at wileyonlinelibrary.com.]

ii. In agreement with intuition, see Figure 2, it is clear how reversion percentage, is temperature dependent, being at 180 °C on average 10–15% higher than that at 150 °C. In addition, having a look into the relationship between the kinetic constant representing reversion in the numerical model (K_3) and experimental reversion % discussed in Discussion and Considerations on the Computed Kinetic Constants section (Figure 25), it appears that K_3-reversion % regression is reasonably linear, with slope roughly temperature independent, but with K_3 values at 180° much higher than those found at 150°.

Finally, it is worth noting that the most important points of innovation of the present research are, from an experimental point of view, a systematic investigation on the role played by two distinct accelerators (TBBS and DPG) on the vulcanizate properties, changing in a wide range both sulfur and accelerators concentrations. It has been found that DPG may help in a considerable reduction of the induction time, but with a considerable increase of reversion and a reduction of the maximum torque, especially at high concentrations. From a numerical point of view, we put at disposal to all practitioners interested, an extremely easy-to-use interactive software that allows determining the kinetic constants of a classic model working well for NR, without any knowledge of operational research and advanced optimization strategies. The reliability of such an interactive software has been demonstrated through comparisons with classic least squares optimization routines.

REFERENCES

1. Milani, G.; Milani, F. *J. Appl. Polym. Sci.* **2012**, *124*, 311.

2. Tanaka, Y. *Rubber Chem. Technol.* **1991**, *64*, 325.

3. Hasenhidl, W. G.; Wolf, S. *Kautsch. Gummi Kunstst.* **1991**, *44*, 118.

4. Coran, A. Y. Science and Technology of Rubber; Academic Press: New York, **1978**; Chapter 7.

5. Leroy, E.; Souid, A.; Sarda, A.; Deterre, R. *Polym. Test.* **2013**; *32*: 575

6. Milani, G.; Milani, F. *J. Appl. Polym. Sci.* **2011**, *119*, 419.

7. Milani, G.; Leroy, E.; Milani, F.; Deterre, R. *Polym. Test.* **2013**, *32*, 1052.

8. Milani, G.; Milani, F. *Polym. Test.* **2014**, *33*, 1.

9. Poh, B. T.; Chen, M. F.; Ding, B. S. *J. Appl. Polym. Sci.* **1996**, *60*, 1569.

10. Poh, B. T.; Tan, E. K. *J. Appl. Polym. Sci.* **2001**, *82*, 1352.

11. Poh, B. T.; Ismail, H.; Tan, E. S. *Polym. Test.* **2002**, *21*, 801.

12. Kamal, M. R.; Sourour, S. *Polym. Eng. Sci.* **1973**, *13*, 59.

13. Ding, R.; Leonov, I. *J. Appl. Polym. Sci.* **1996**, *61*, 455.

14. Ding, R.; Leonov, I.; Coran, A. Y. *Rubber Chem. Technol.* **1996**, *69*, 81.

15. Han, I. S.; Chung, C. B.; Kang, S. J.; Kim, S. J.; Chung, H. C. *Polymer (Korea)* **1998**, *22*, 223.

16. Colin, X.; Audouin, L.; Verdu, J. *Polym. Degrad. Stabil.* **2007**, *92*, 906.

17. Milani, G.; Hanel, T.; Milani, F.; Donetti, R. *J. Math. Chem.* **2015**, *53*, 975.

18. Milani, G.; Milani, F. *J. Math. Chem.* **2015**, *53*, 1363.

19. Prigogine, I. Self-organization in Non-equilibrium Systems, from Dissipative Structure to Order to Fluctuations; Wiley: NY, **1977**.

20. Milani, G.; Milani, F. NR Sulphur Vulcanization: Interaction Study between TBBS and DPG by means of a Combined Experimental Rheometer and Meta-Model Best Fitting Strategy; submitted.

21. ASTM D3184 – 11. Standard Practice for Rubber—Test Formulas, Mixing Procedures, and Test Methods for the Evaluation and Production Control of Natural Rubber (NR); ASTM **2011**.

22. Milani, G.; Milani, F. Freeware Graphical User Interface Software based on Han's Model for the Rapid Determination of Kinetic Constants in NR Vulcanized with Sulphur; submitted.

23. Sun, X.; Isayev, A. I. *Rubber Chem. Technol.* **2009**, *82*, 149.

24. Akiba, M.; Ashim, A. S. *Prog. Polym. Sci.* **1997**, *22*, 475.